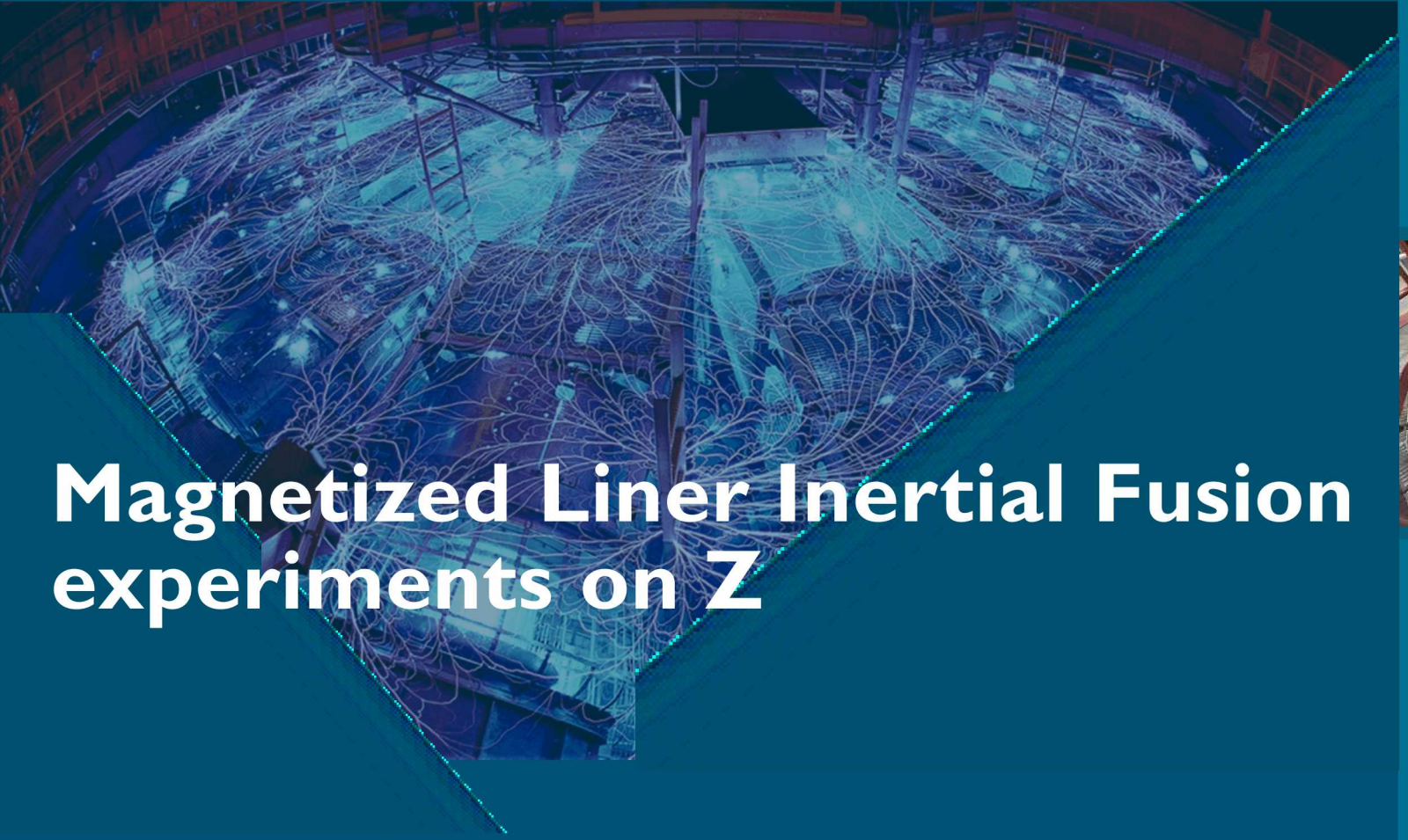

Magnetized Liner Inertial Fusion experiments on Z

SAND2019-8174PE

PRESENTED BY

Dave Ampleford and Pat Knapp

Seminar at First Light Fusion,

July 12th, 2019

Sandia National Laboratories is a multimission laboratory managed and operated by National Technology & Engineering Solutions of Sandia, LLC, a wholly owned subsidiary of Honeywell International Inc., for the U.S. Department of Energy's National Nuclear Security Administration under contract DE-NA0003525.

MagLIF is a major effort at Sandia, involving a large group of researchers

This work performed in collaboration with:

- M. R. Gomez, A.J. Harvey-Thompson, E. C. Harding, M. R. Weis, C. A. Jennings, S. A. Slutz, M. Geissel, J. R. Fein, M. Glinsky, T. Moore, J. L. Porter, P. Rambo, D. E. Ruiz, J. Schwarz, J. E. Shores, I. C. Smith, C. S. Speas, G. A. Chandler, K. D. Hahn, C.R. Ruiz, M. Mangan, S. B. Hansen, D.C. Lamppa, L. Lucero, R. Paguio, L. Perea, G. Robertson, G. E. Smith, K. Whittemore, G. A. Rochau, K. J. Peterson, D. B. Sinars

- A large group of scientists, engineers and technologists that support every shot on Z!

Overview:

What is MagLIF

Instabilities in MagLIF

Reducing instability seeds and better reproducibility

Diagnostics and analysis techniques are key to further developments

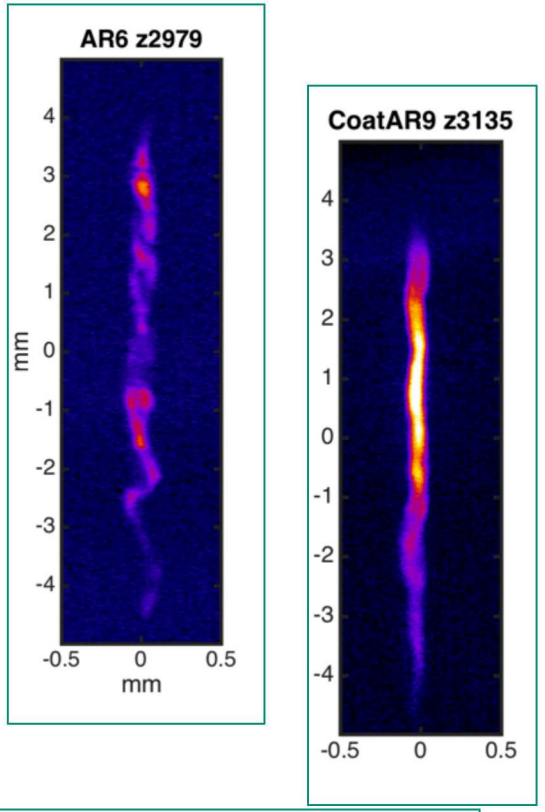

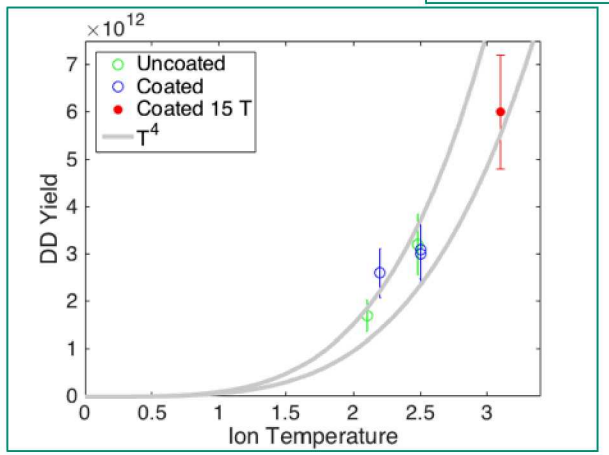

Magneto-inertial fusion requires magnetic fields to trap charged fusion products

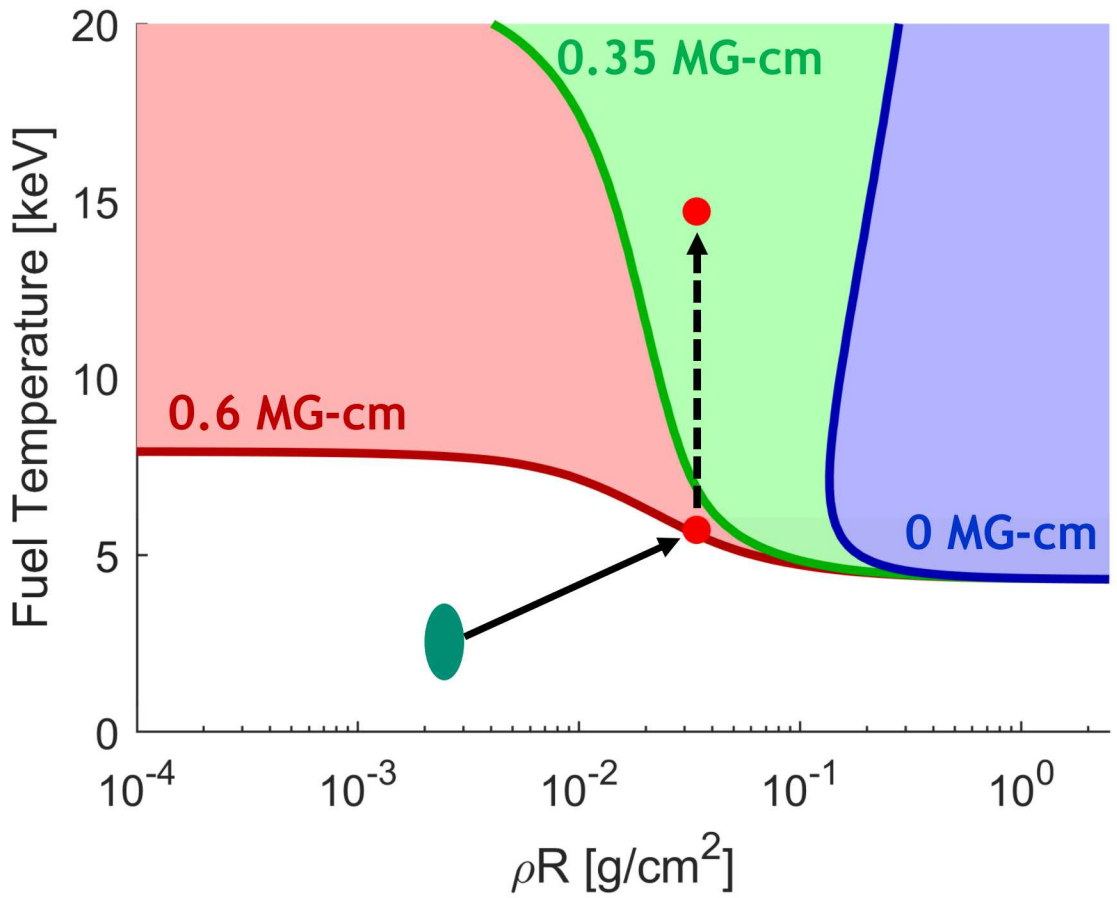

Ignition-scale MIF designs achieve self-heating through magnetically-trapped charged fusion products

- Effective fuel areal density is too small for most DT-alphas to deposit energy
  - Low fuel density
  - Cylindrical convergence → density ~ $1/R^2$
  - Relatively small radius
- Large magnetic fields trap charged fusion products opening up a larger ignition space

When the magnetic field-radius product (BR) ~0.3 MG-cm, the Larmor radius of fusion alphas is approximately the fuel radius

Background: Magnetized Liner Inertial Fusion uses a pulsed power driver to implode a low Z liner (tube) of pre-heated pre-magnetized fusion fuel

Imploding
Be tube
or "liner"

Gaseous
D_2 fuel
0.7 mg/cc

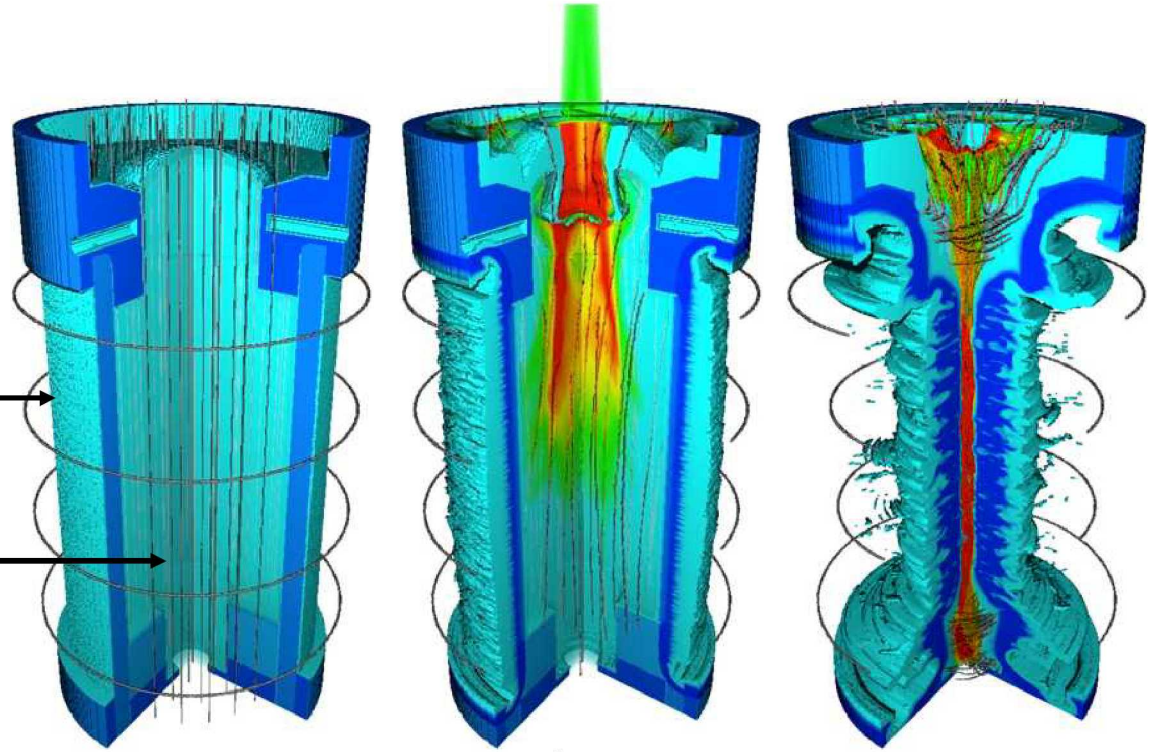

Magnetization
B = 10 T

Laser
Heating

Compression

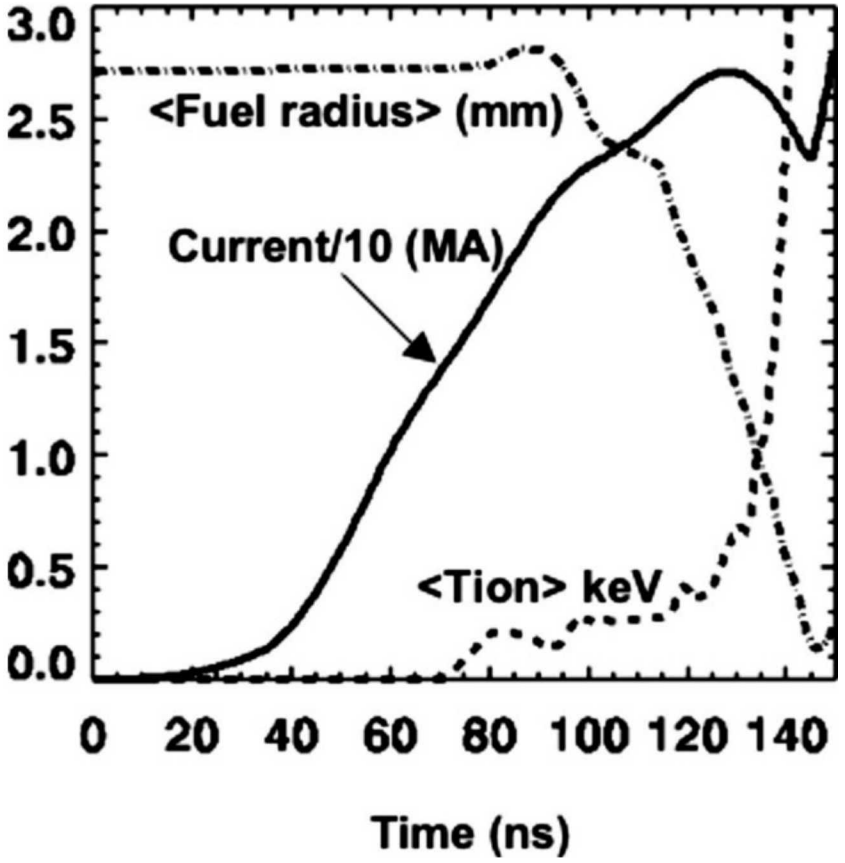

S.A. Slutz *et al.*, Physics of Plasmas
M.R. Gomez *et al.*, Phys. Rev. Lett.

Background: Magnetized Liner Inertial Fusion uses a pulsed power driver to implode a low Z liner (tube) of pre-heated pre-magnetized fusion fuel

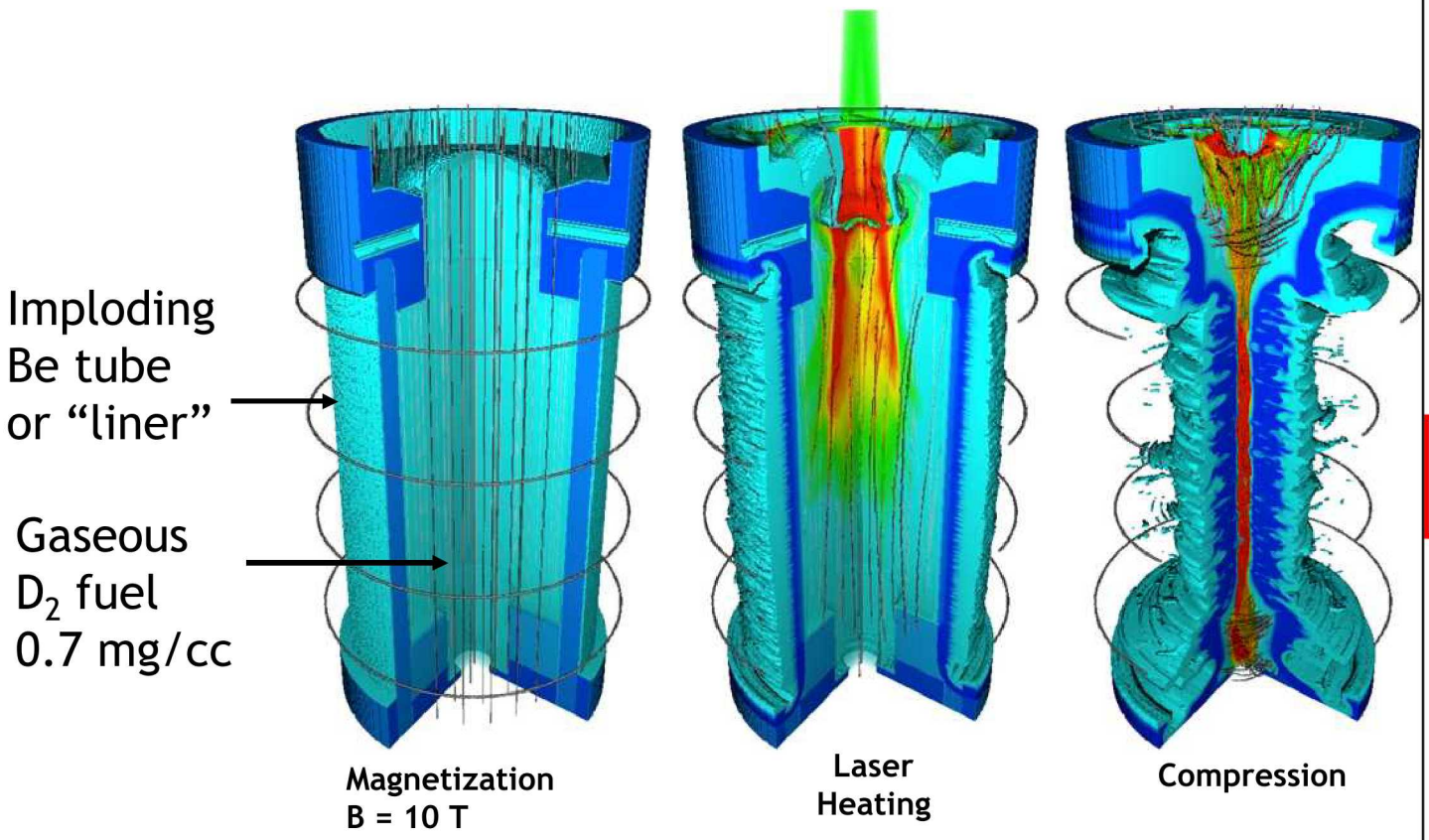

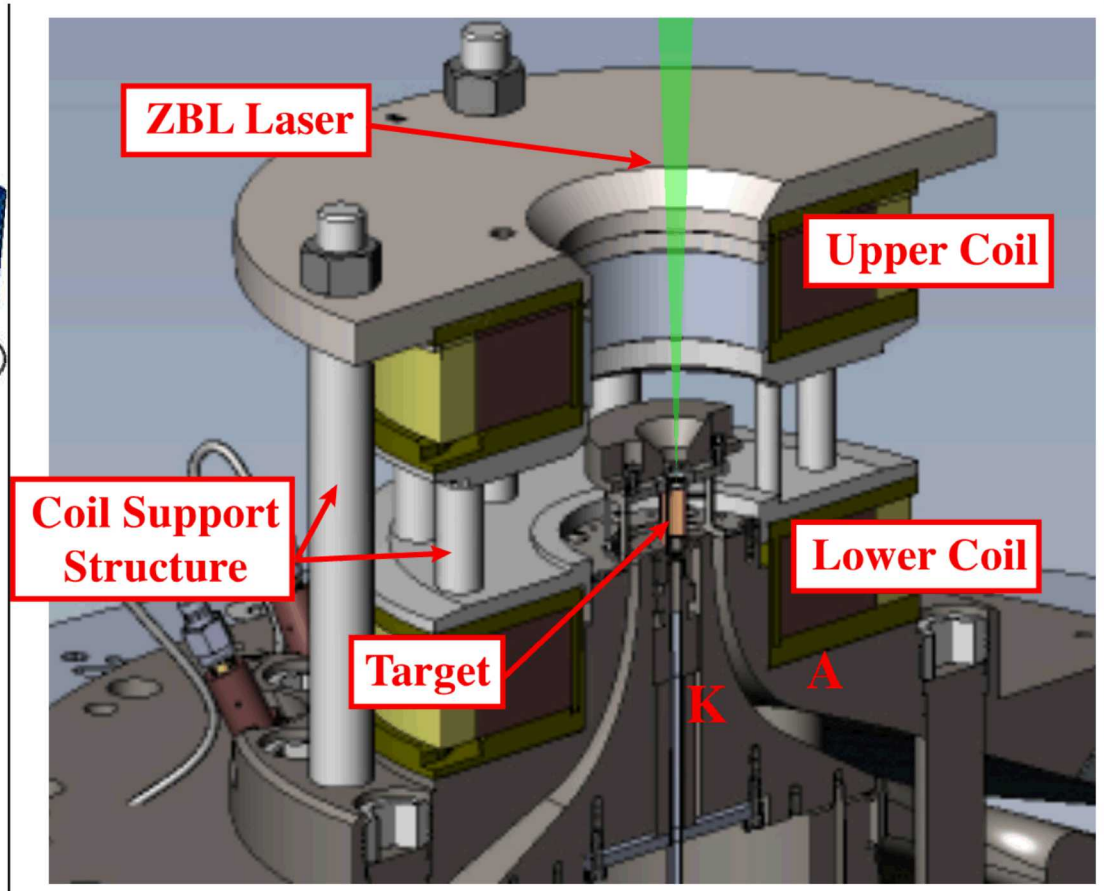

Background: Magnetized Liner Inertial Fusion uses a pulsed power driver to implode a low Z liner (tube) of pre-heated pre-magnetized fusion fuel

MagLIF experiments have demonstrated the necessary components of magneto-inertial fusion, and achieved primary n_{DD} yields ~10^{12} - 10^{13}

Imploding Be tube or "liner"

Gaseous D_2 fuel 0.7 mg/cc

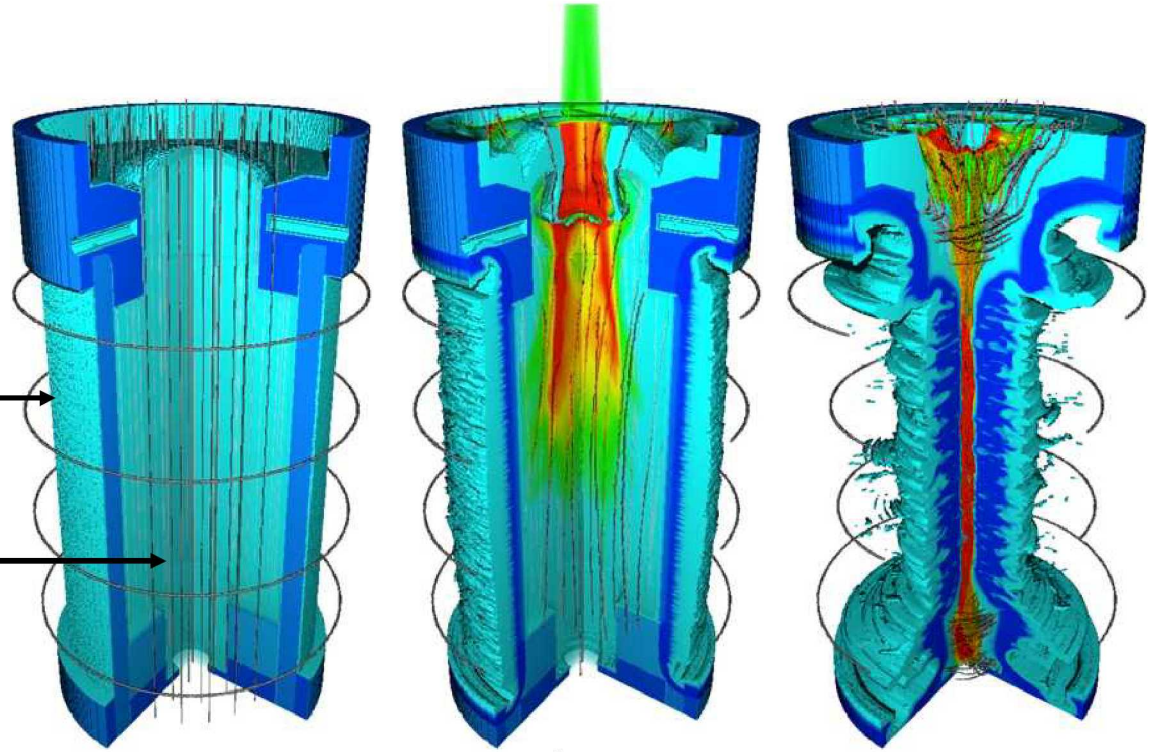

Magnetization B = 10 T

Laser Heating

Compression

	No B-field	B-field
No Laser	3e9	1e10
Laser	4e10	2e12

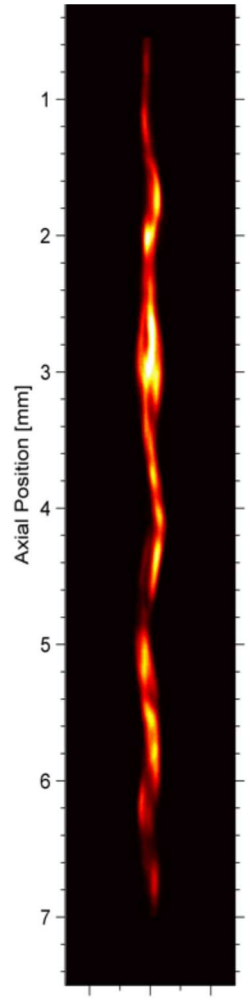

MagLIF stagnations exhibit complex helical structures

We have observed helical structures early in time in pre-magnetized liners Various theories exist to explain these structures

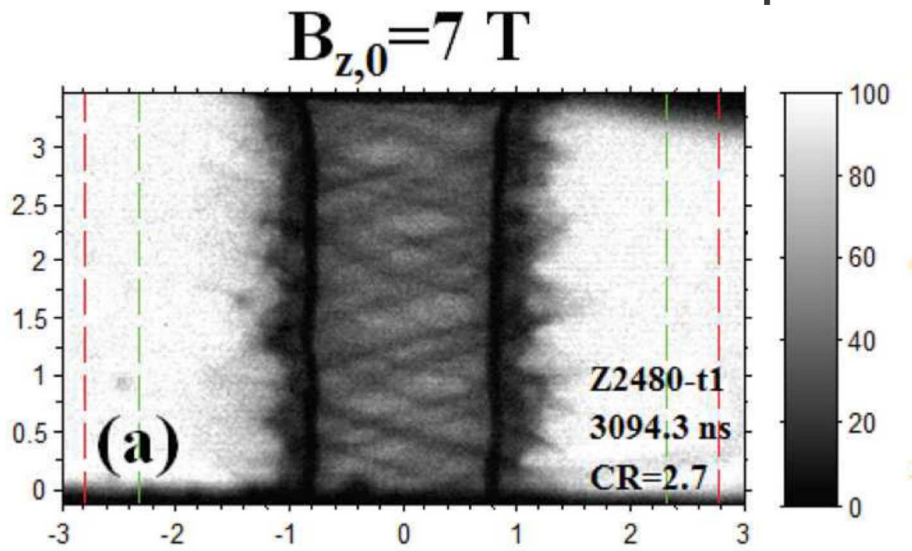

In radiography experiments of premagnetized liners we see a helical structure

- We can't presently radiograph experiments with preheat

T.J. Awe *et al.*,
Physics of Plamsas 21, 056303 (2014)

There are a number of proposed explanations for these helical structures

- Electrons streaming onto liner surface (Sefkow *et al.*)
- Force free current paths on the liner surface (Velikovich)
- Compression of field by low density feed plasma (Seyler, Martin, Hamlin, Physics of Plasmas 25, 062711 (2018)

3D simulations indicate that these instabilities degrade yield

- Estimated to be 40% effect at present, deteriorates with increasing field, current
- Increase fuel density an preheat energy helps slightly by reducing convergence, but present capabilities won't outweigh field/current impacts

We can design experiments to test if this instability feeds through to the stagnation column

Data indicate that these helical structures at stagnation are the result of early-time helical mode imprinted on the outer surface of the liner

We can control feedthrough of instabilities from the outer surface of the liner

- Aspect ratio will dictate the feedthrough
  - $\mathrm{AR} = \frac{Outer\ Radius}{Wall\ Thickness}$
  - Lower aspect ratios will be more robust to feedthrough
    (e.g. AR4.5)

By testing this on Z we have demonstrated that stagnation structures are consistent with feedthrough

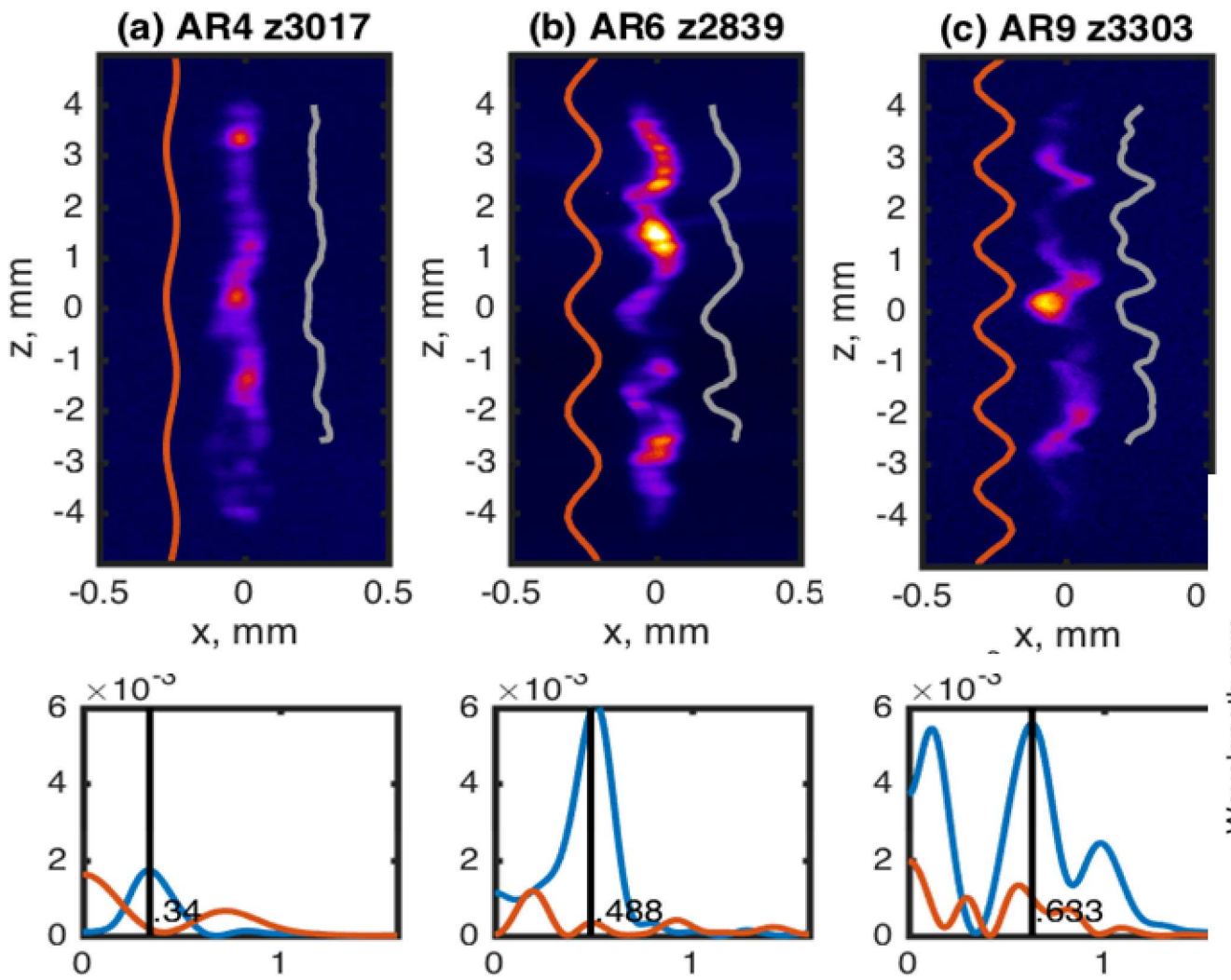

We can control feedthrough of instabilities from the outer surface of the liner
Aspect ratio will dictate the feedthrough
AR = Outer Radius / Wall Thickness
Lower aspect ratios will be more robust to feedthrough
(e.g. AR4.5)
By testing this on Z we have demonstrated that stagnation structures are consistent with feedthrough

Data indicate that these helical structures at stagnation are the result of early-time helical mode imprinted on the outer surface of the liner

We can control feedthrough of instabilities from the outer surface of the liner

- Aspect ratio will dictate the feedthrough
  - $\mathrm{AR} = \frac{Outer\ Radius}{Wall\ Thickness}$
  - Lower aspect ratios will be more robust to feedthrough
    (e.g. AR4.5)

By testing this on Z we have demonstrated that stagnation structures are consistent with feedthrough

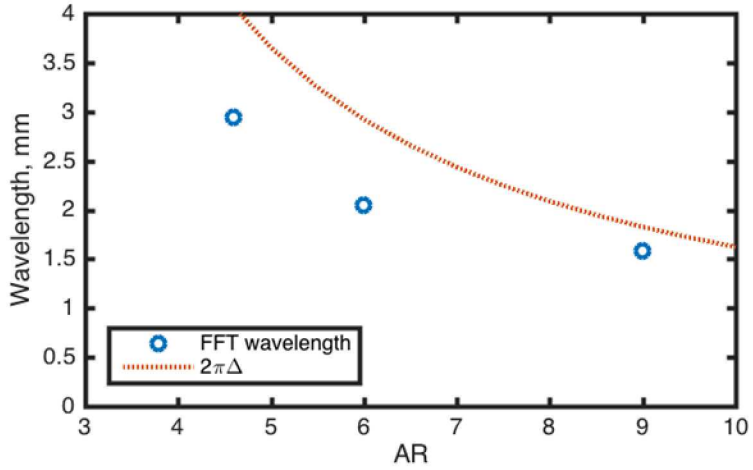

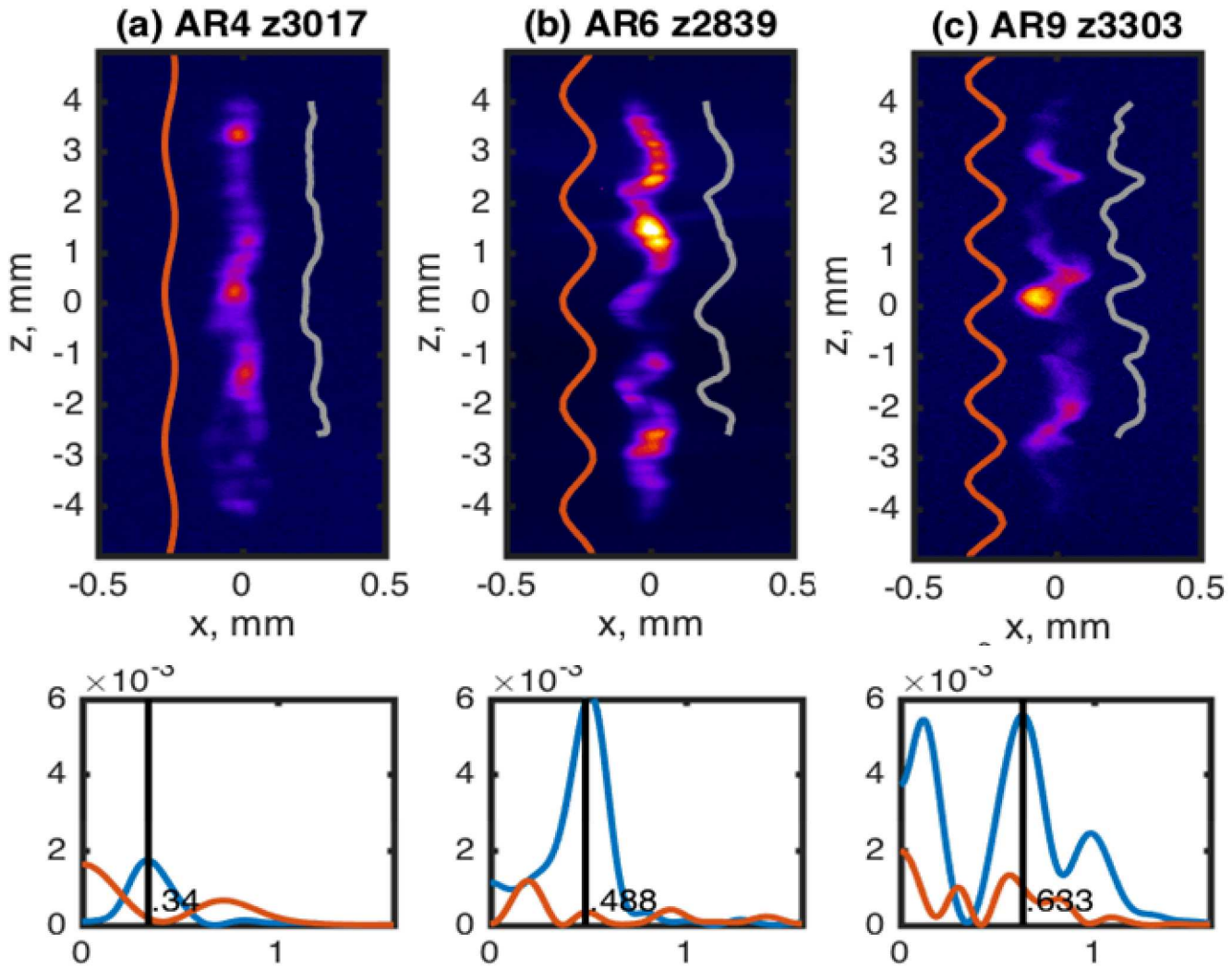

We can significantly reduce the seed of these instabilities

We believe the seed for the helical instability is electro-thermal instability – if it is then theory shows we can fix it

Modeling

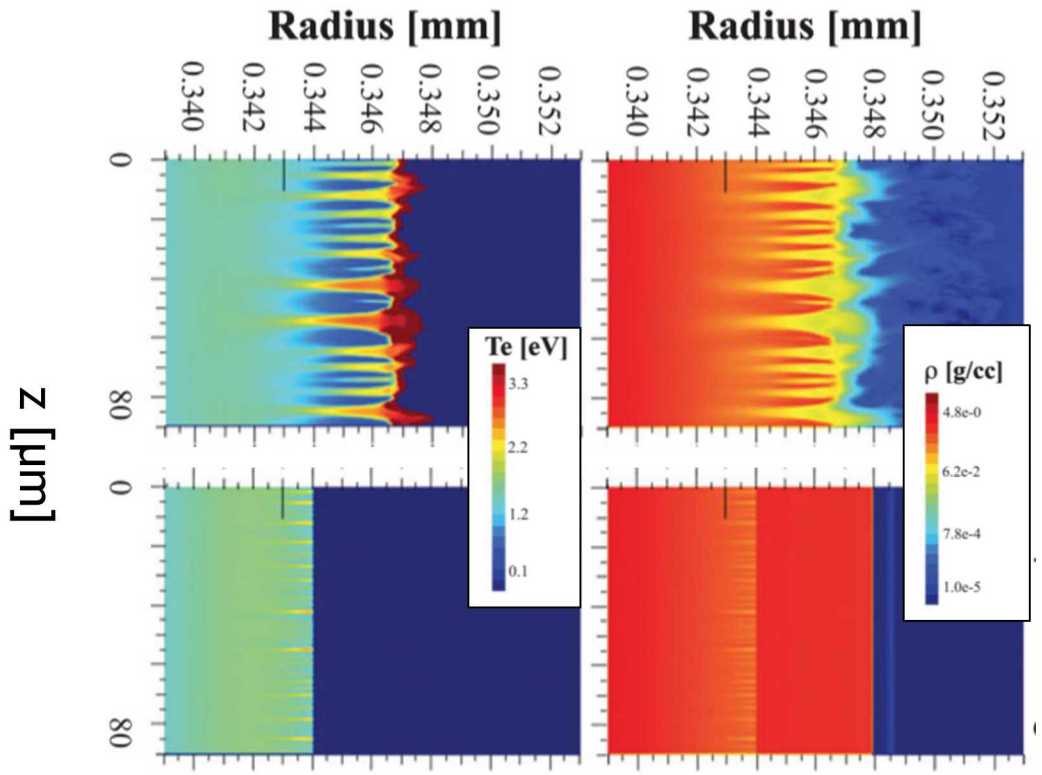

Experiments (AR6)

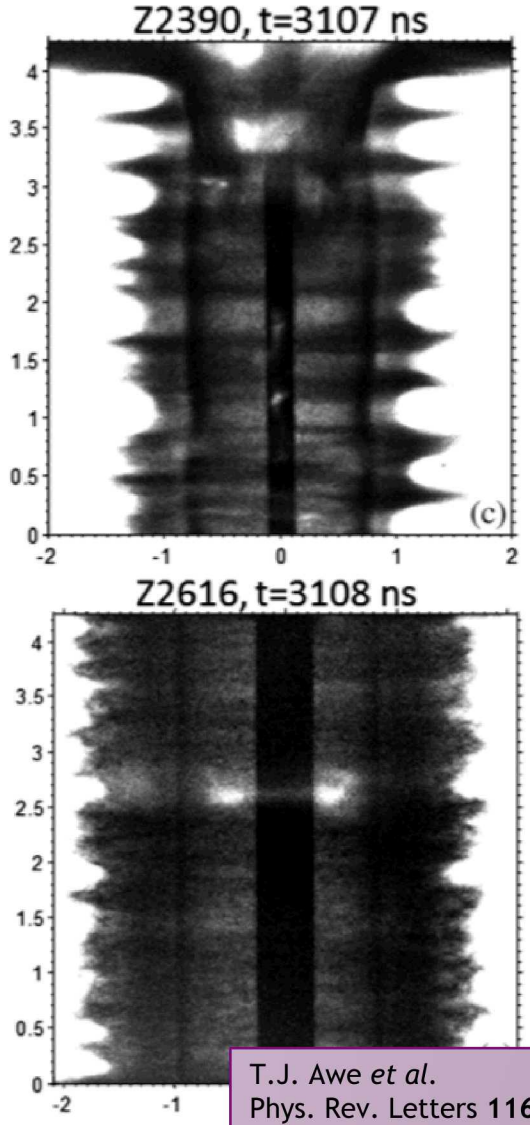

Uncoated

Coated

K.J. Peterson *et al.*,
Phys. Rev. Letters **112**, 135002 (2014)

T.J. Awe *et al.*
Phys. Rev. Letters **116**, 065001 (2016)

Late in time data indicates very good implosion stability with coatings

AR9 data

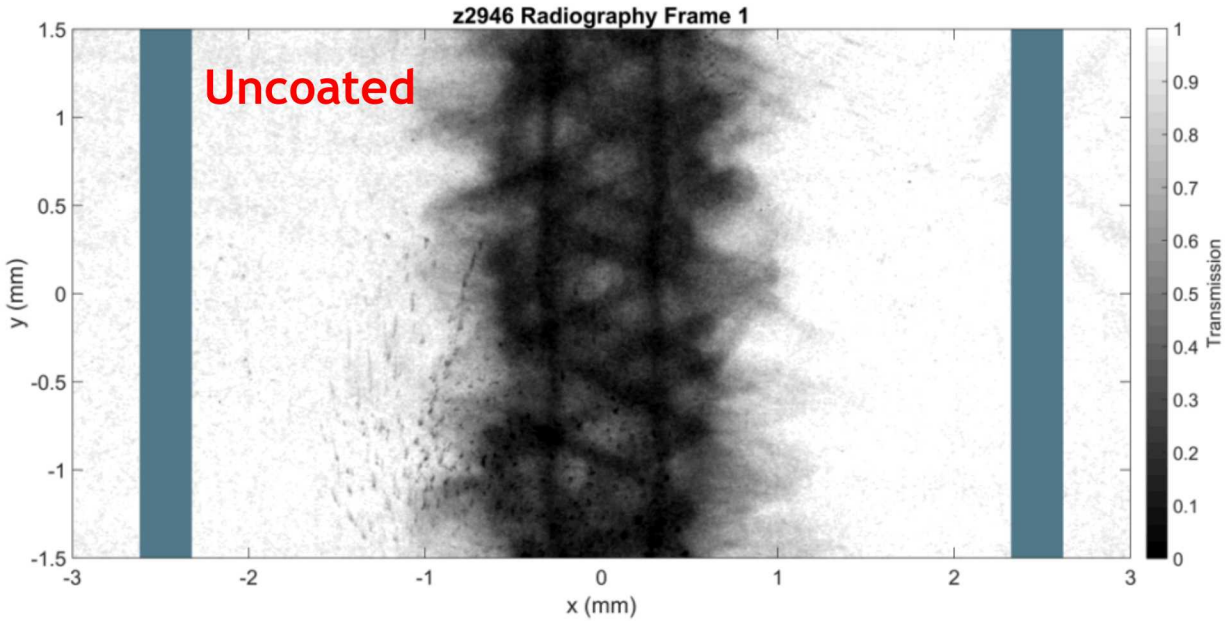

Stability looks good at very late time

- Convergence ratio ~ 17

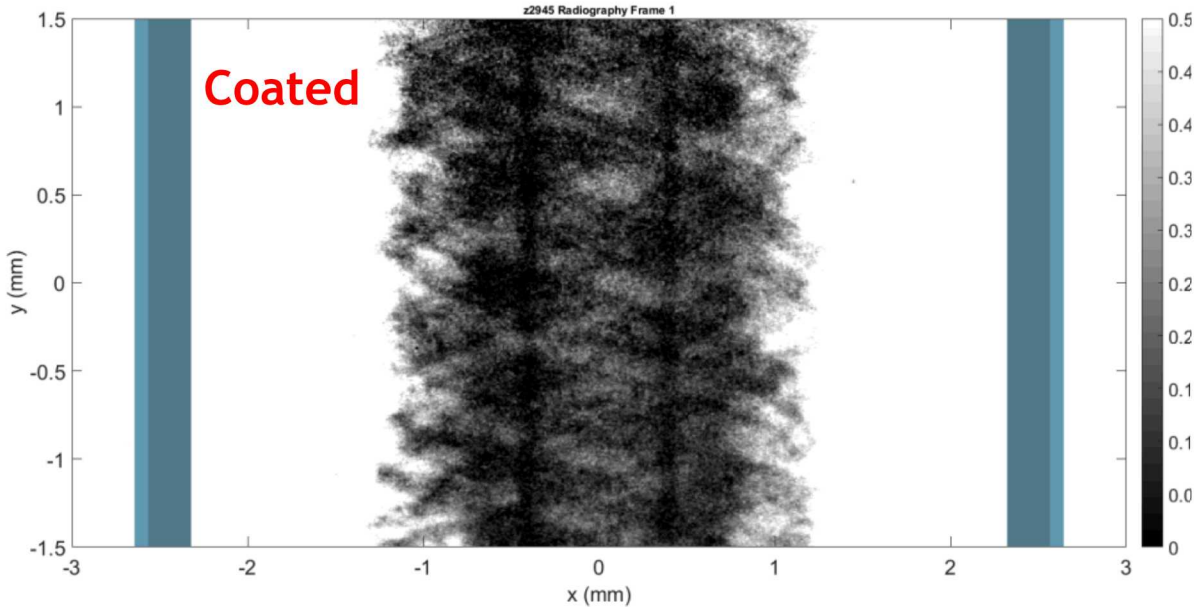

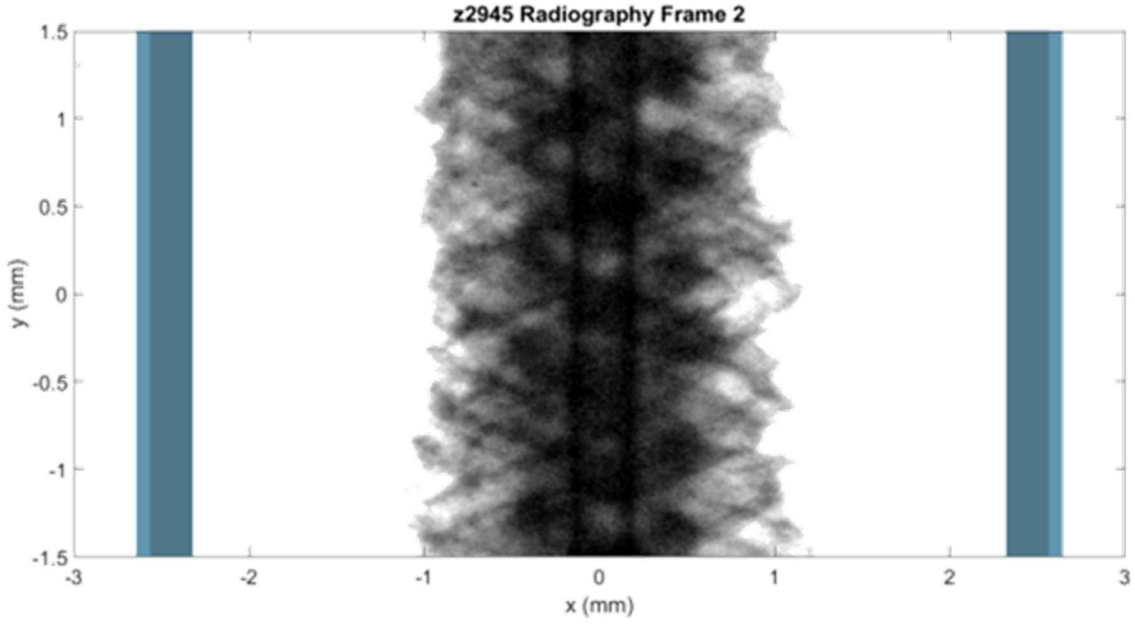

Over multiple shots we get similar stagnation morphologies

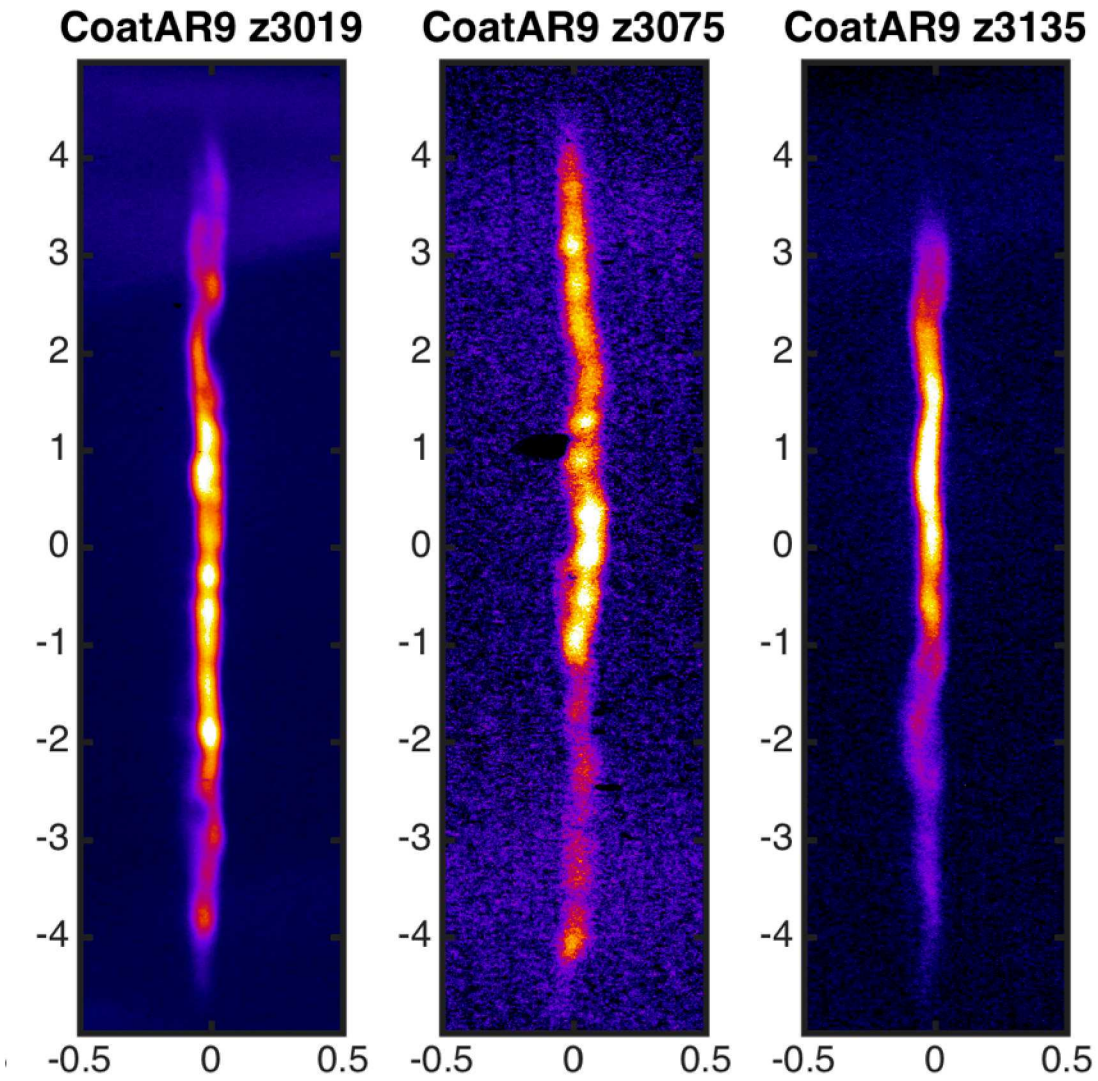

Taking the coated AR9 implosion thought to stagnation (i.e. now with preheat) we find we obtain a uniform stagnation column

- >4 mm of bright, continuous x-ray emission
- Minimal (if any) residual helical structure

Over multiple experiments we obtain reasonably uniform stagnations

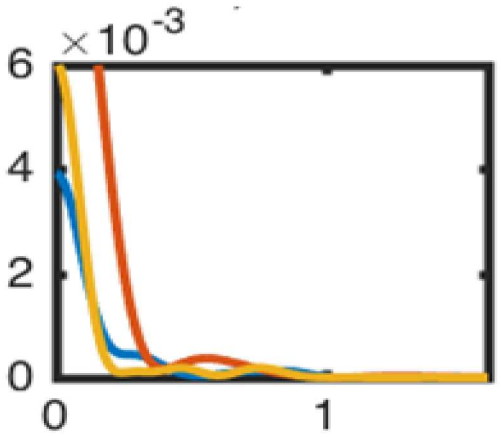

Of course, there's more to stagnation than an image

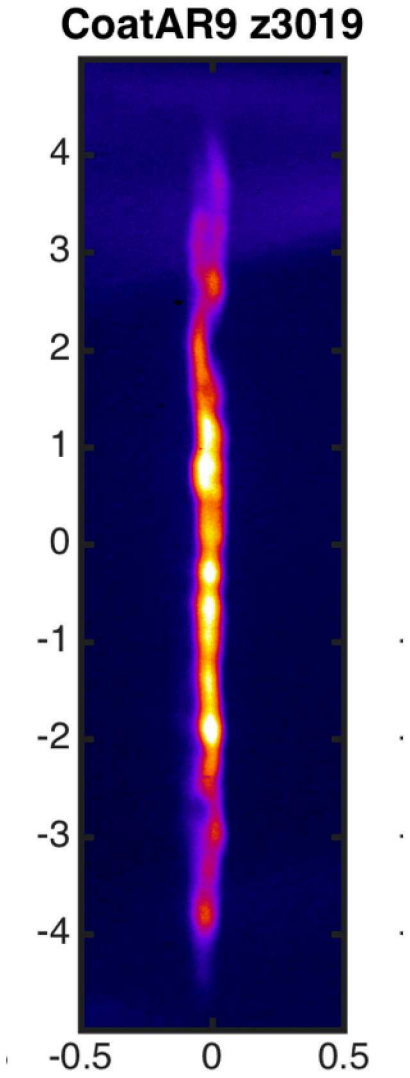

- Neutron structure
- Neutron spectrum (nTOF) (ion temperature, magnetization)
- X-ray emissivity
- Primary DD yield
- Secondary DT yield
- Time resolved structure
- Electron temperature

The axial neutron emission structures look uniform

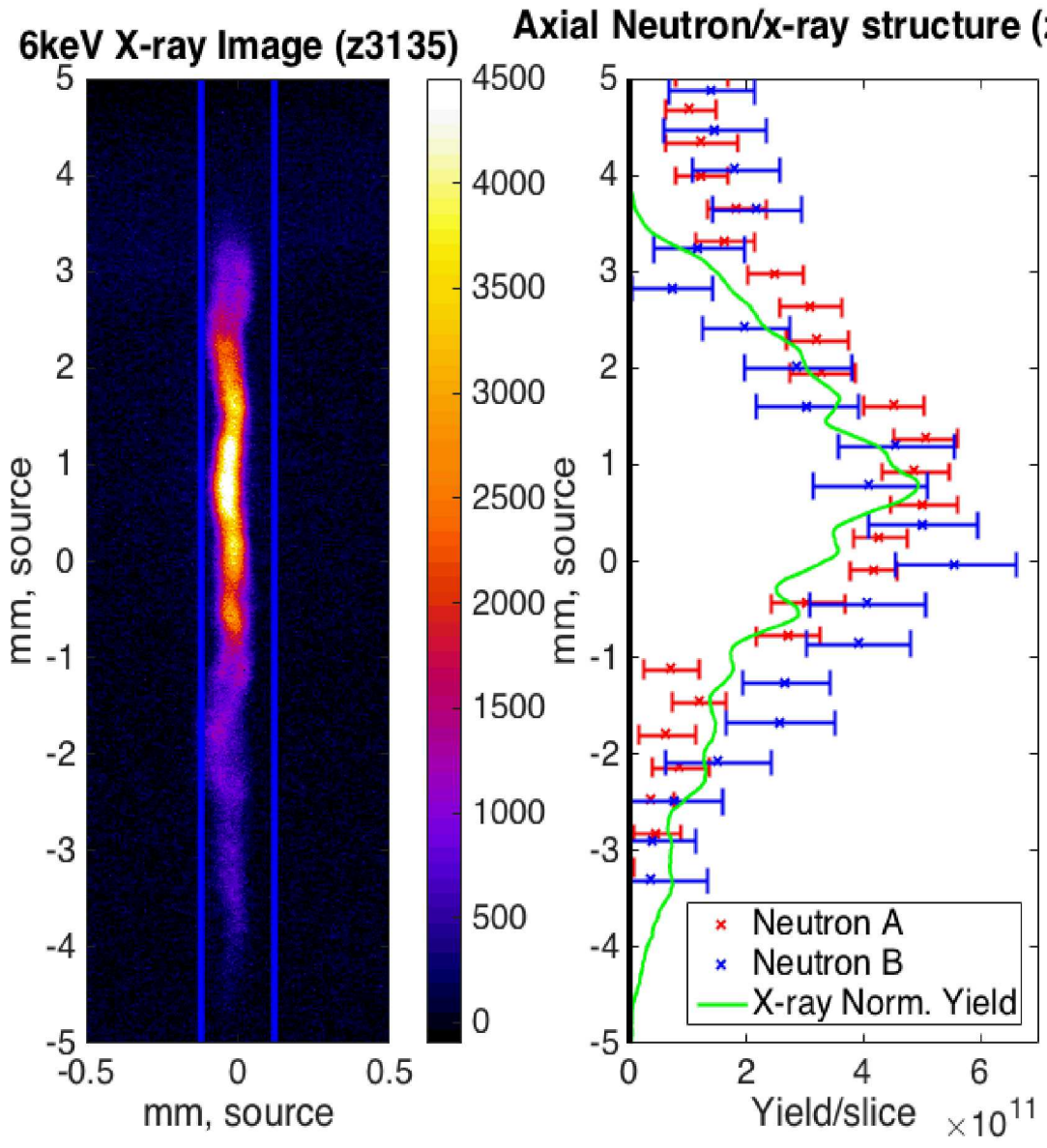

We recently developed a one-dimensional neutron imager for Z

- Uses tungsten rolled edge slit to image onto CR39

Initial data indicates the neutron emitting regions is also quasi-uniform

- For this case good correlation between neutron and x-ray emitting regions

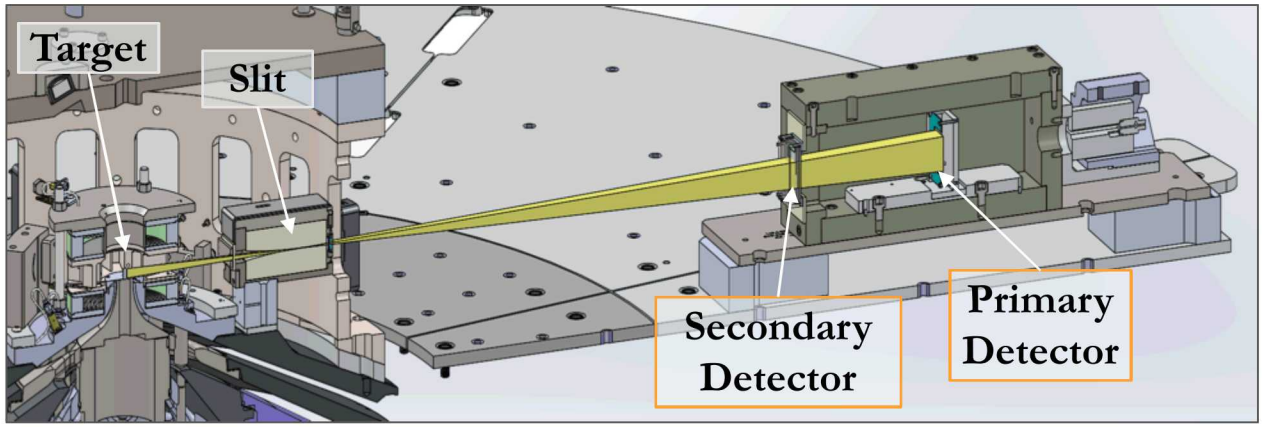

J.D. Vaughan *et al.*, Rev. Sci. Instrum. **89**, 10I121 (2018)
D.J. Ampleford *et al.*, Rev. Sci. Instrum. **89**, 10I132 (2018)
See posters: **GP11.00132** (Vaughan), **GP11.00094** (Ampleford)

We have recently developed a time-resolved imaging capability for MagLIF: For AR6 stagnations we see very non-uniform stagnation

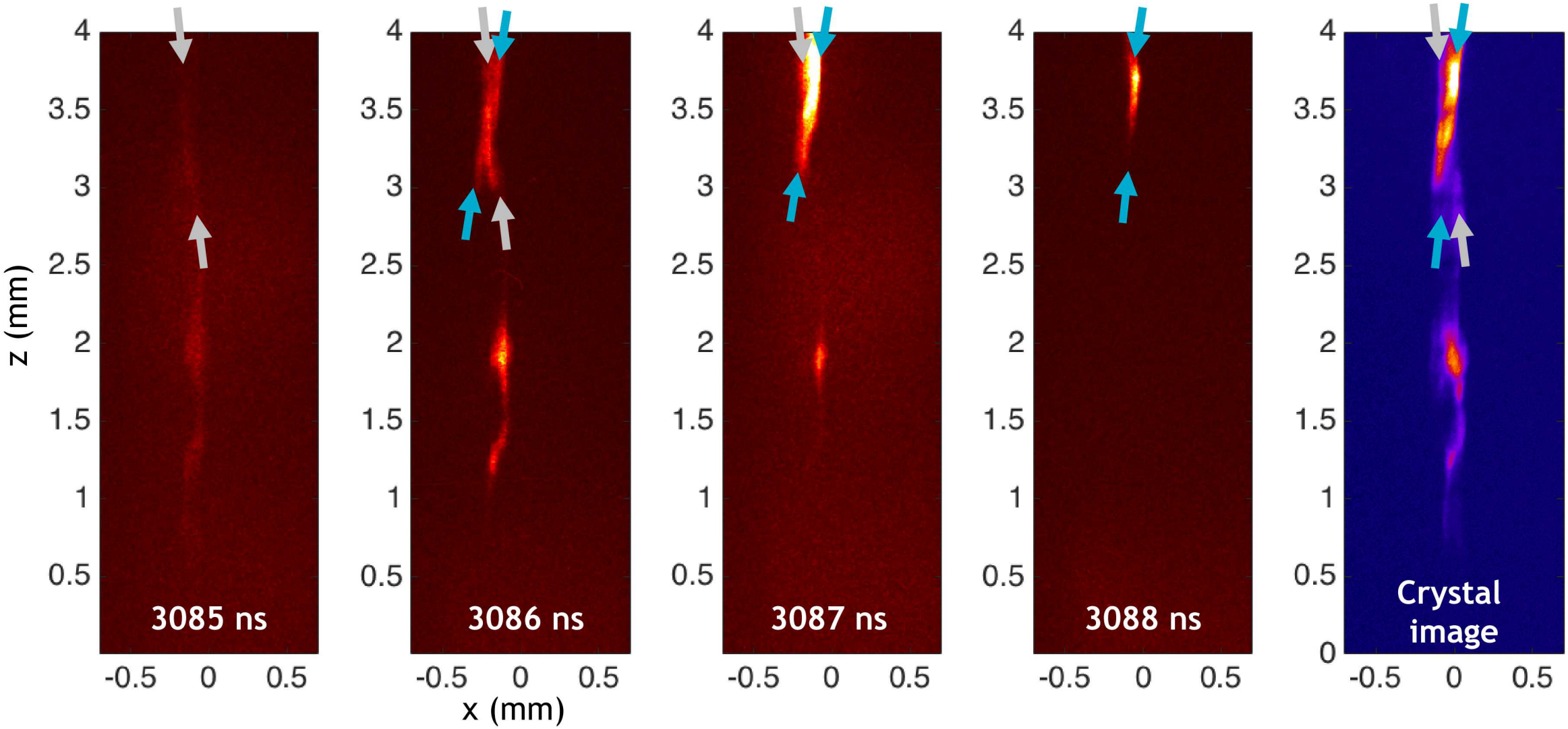

TiGHER Pinhole Camera:
Developed by T. Webb *et al.*

With Coated AR9 liners we see a significantly more uniform stagnation over time

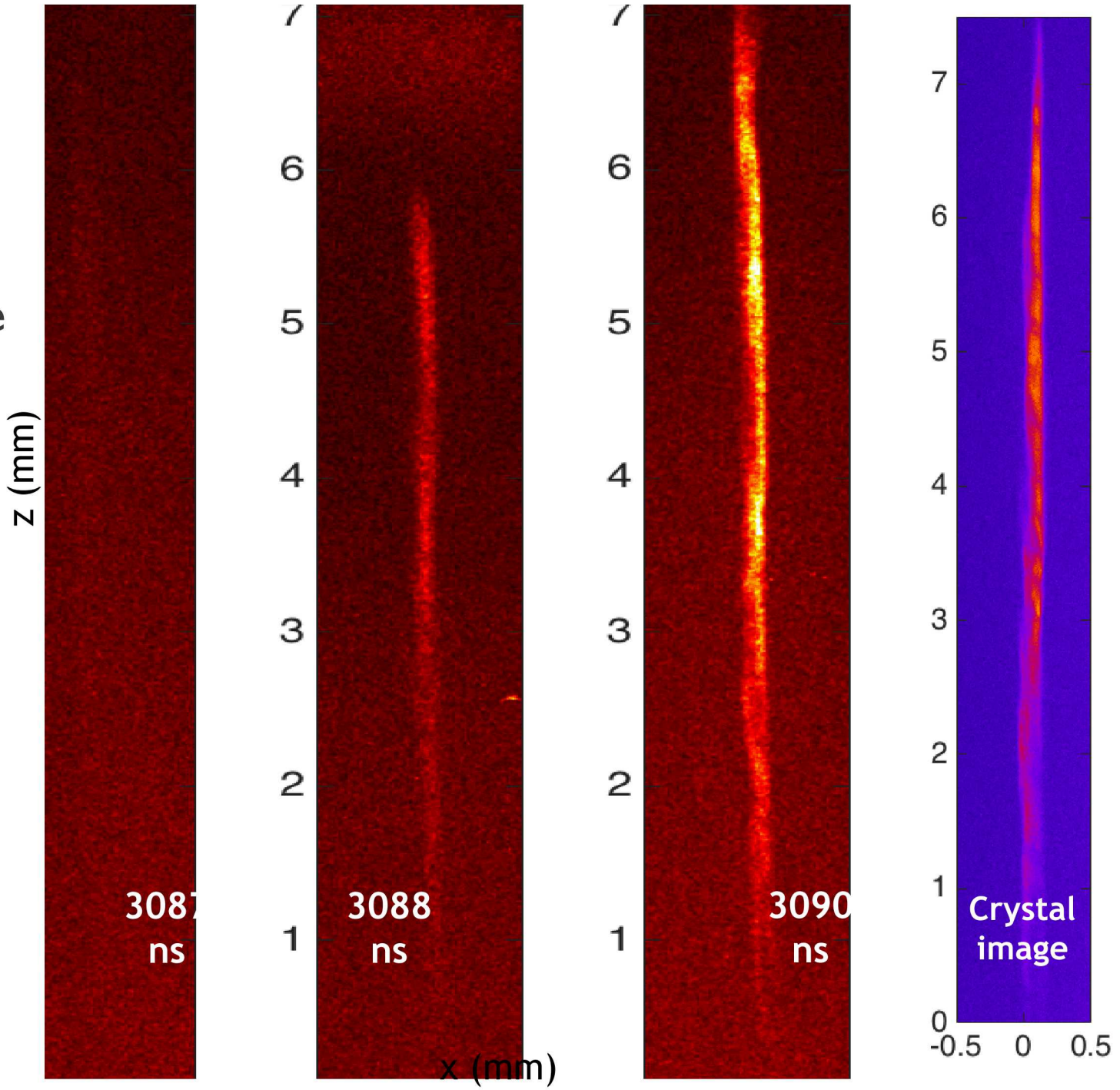

TiGHER Pinhole Camera:
Developed by T. Webb *et al.*

We can use the spectrum of the secondary DT neutrons as a diagnostic of magnetization at stagnation

AR6 data

Magnetic field consistent with flux compression

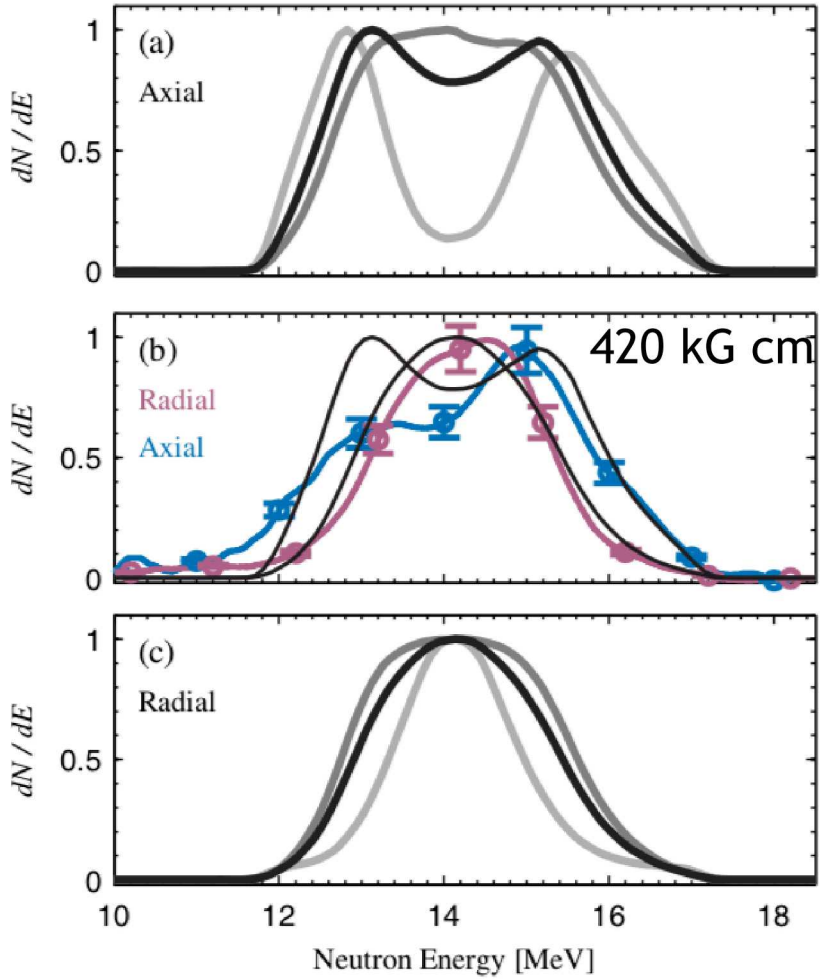

Relationship between DT and DD yield varies with magnetization

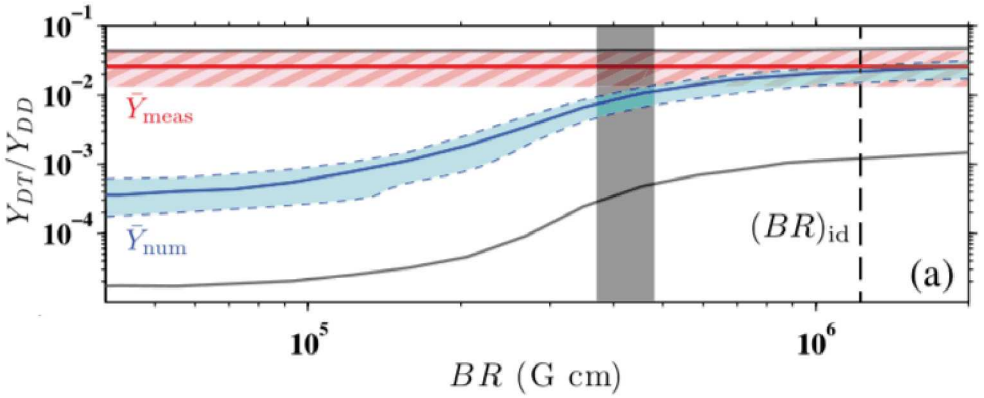

P.F. Schmit *et al.*, Phys. Rev. Lett

For the coated high aspect ratio liners we have very clean measures of magnetization at stagnation

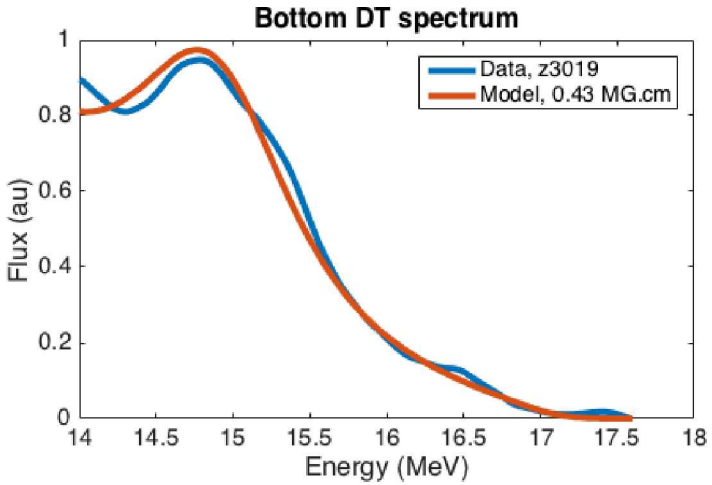

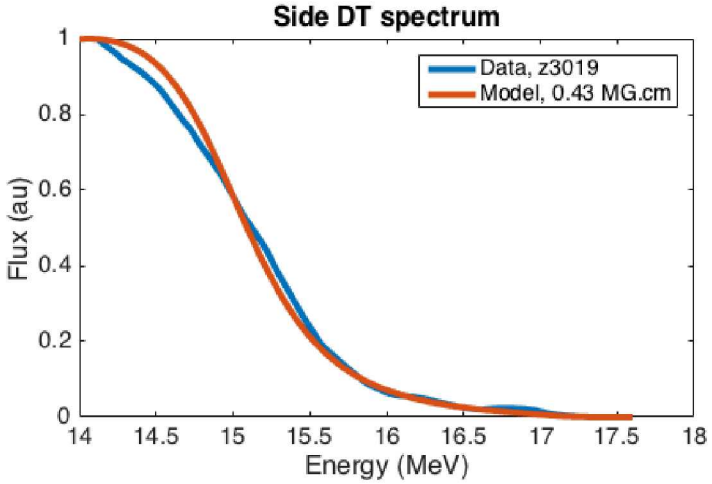

Analysis method based on
P.F. Schmit *et al.*, Phys. Rev. Lett

For AR9 dataset

- Both BR diagnostics indicate BR ~ 400 kG.cm
- This is on the high end of the BR from the AR6 dataset
  - Better than best performing AR6 shots
- Agreement between two metrics is better than for AR6

For coated AR9 setup we have shown assumption of long neutron producing region is valid

Coated AR9 data

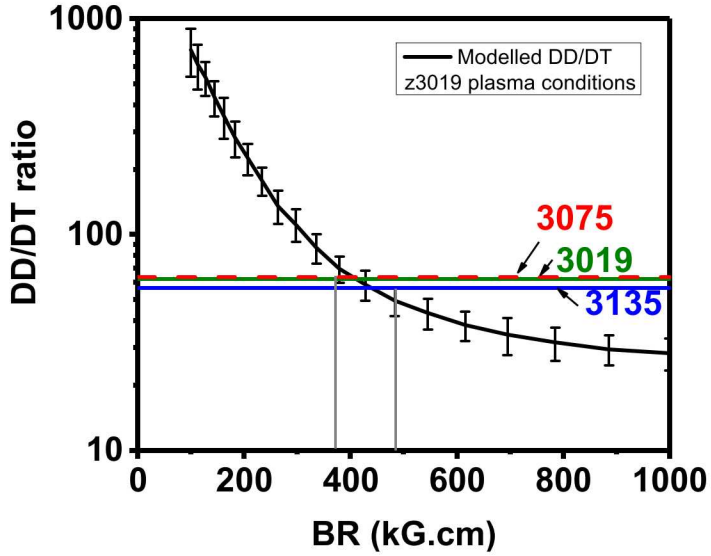

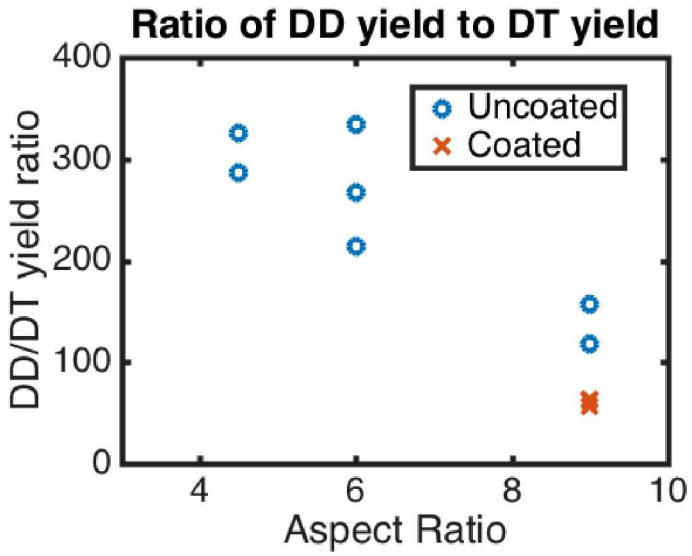

Many key stagnation parameters, including yield, are reproducible

These three, nominally identical coated AR9 experiments have exhibited very similar behavior

- Similar Primary DD yields
- Similar Ion temperatures
- Similar DT yields

While going to the coated AR9 platform hasn't improved MagLIF performance

- Performance hasn't been diminished
- Reproducibility is better

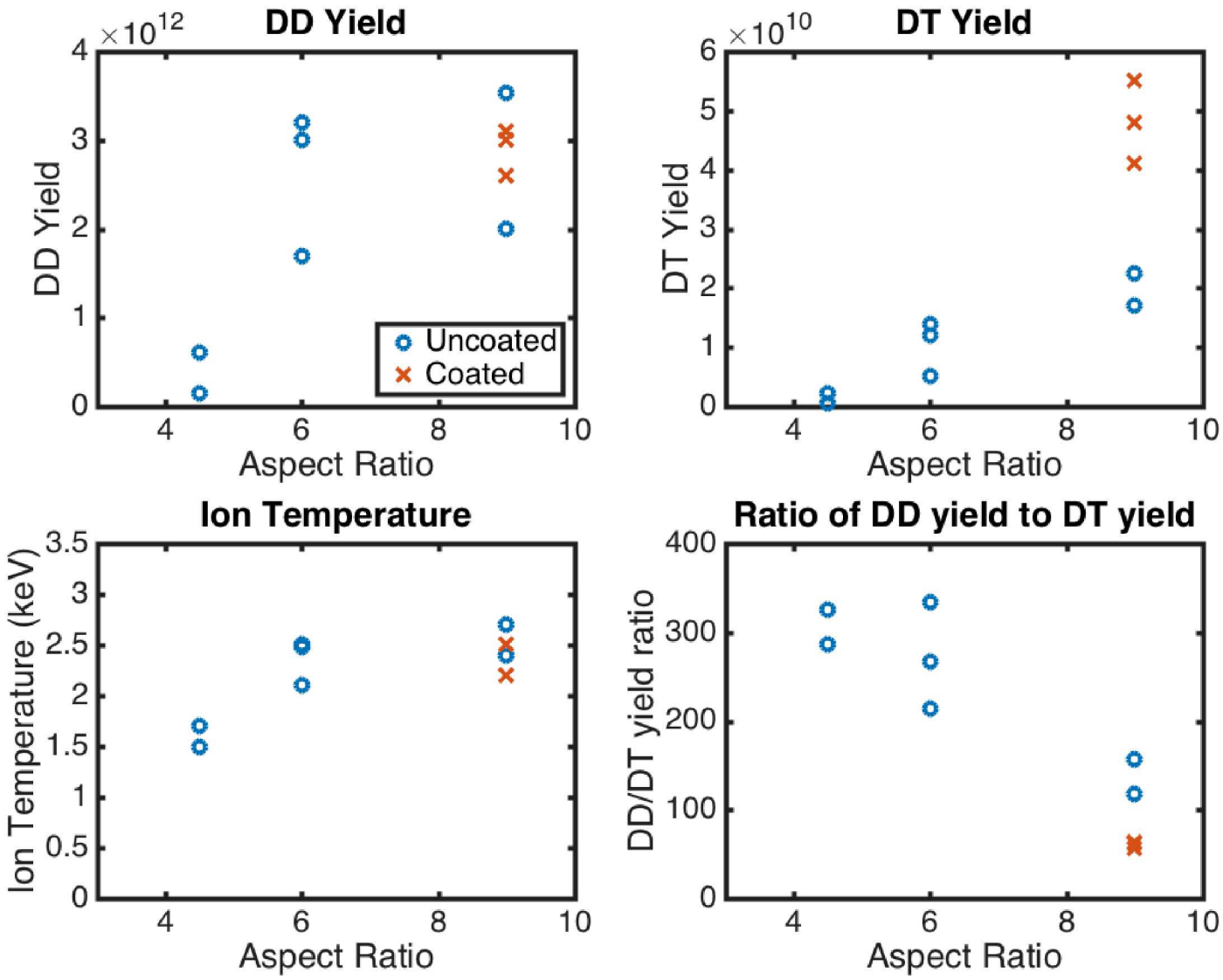

This 15T experiment also demonstrated scaling with ion temperature

Significant enhancement in ion temperature is matched by significant change in DD yield

Within uncertainties in yield, data is following T^4 scaling

In a parallel effort, this coated AR9 platform is being used to study new preheat platforms

- See next talk by Adam Harvey-Thompson

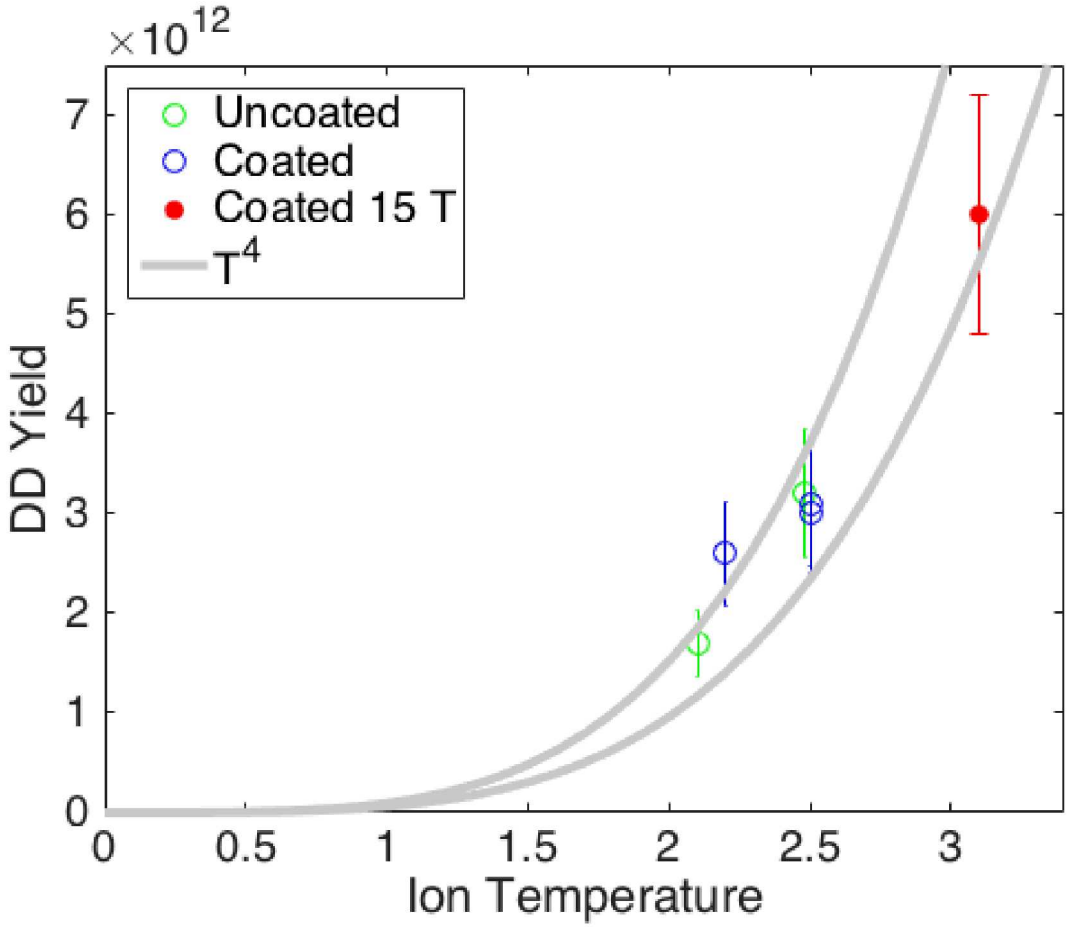

By continual improvements and optimization MagLIF has a lot of potential on Z and on future generators

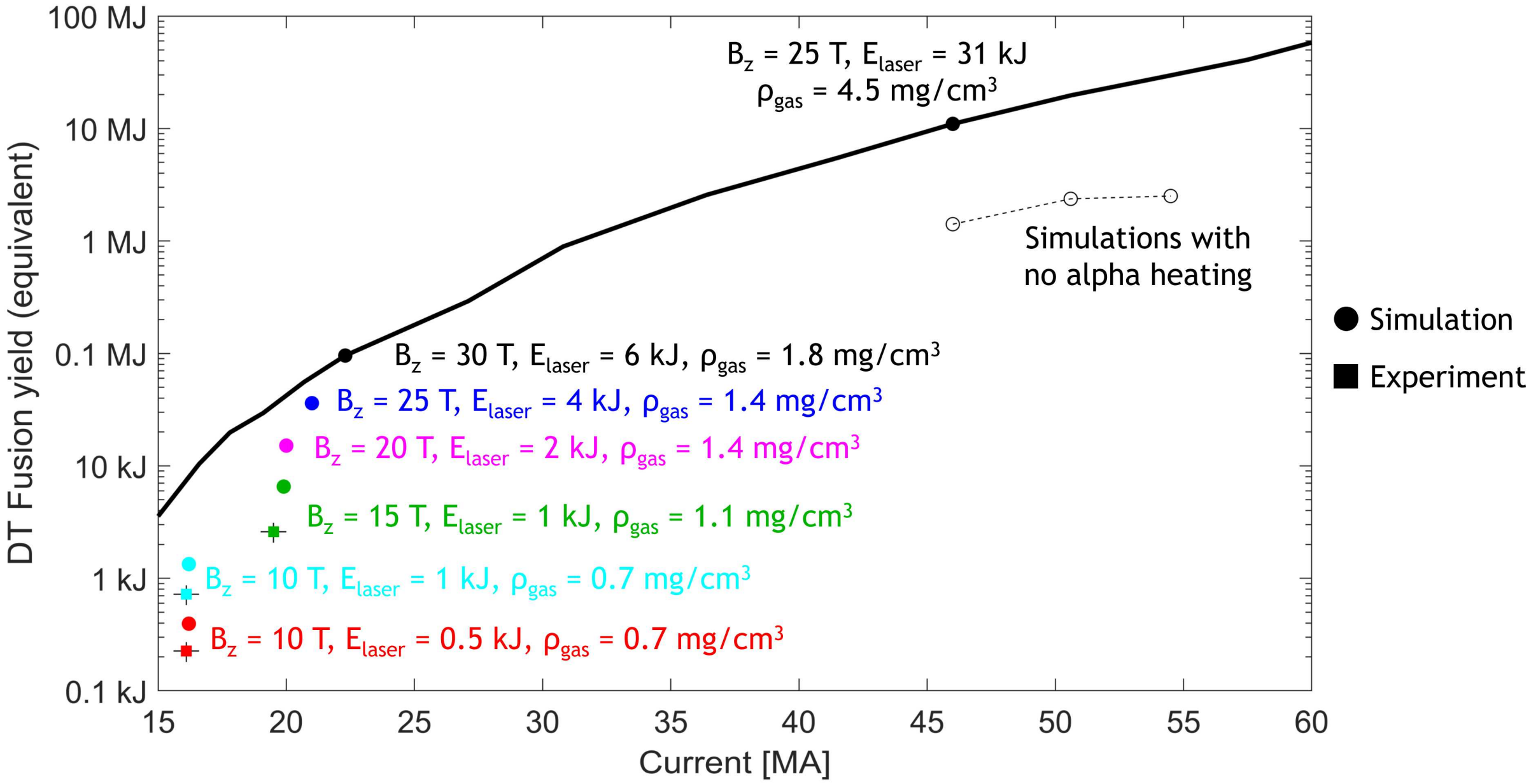

Bayesian analysis of MagLIF experiments

We have developed a forward model that allows direct, quantitative comparison of the data with synthetic diagnostics

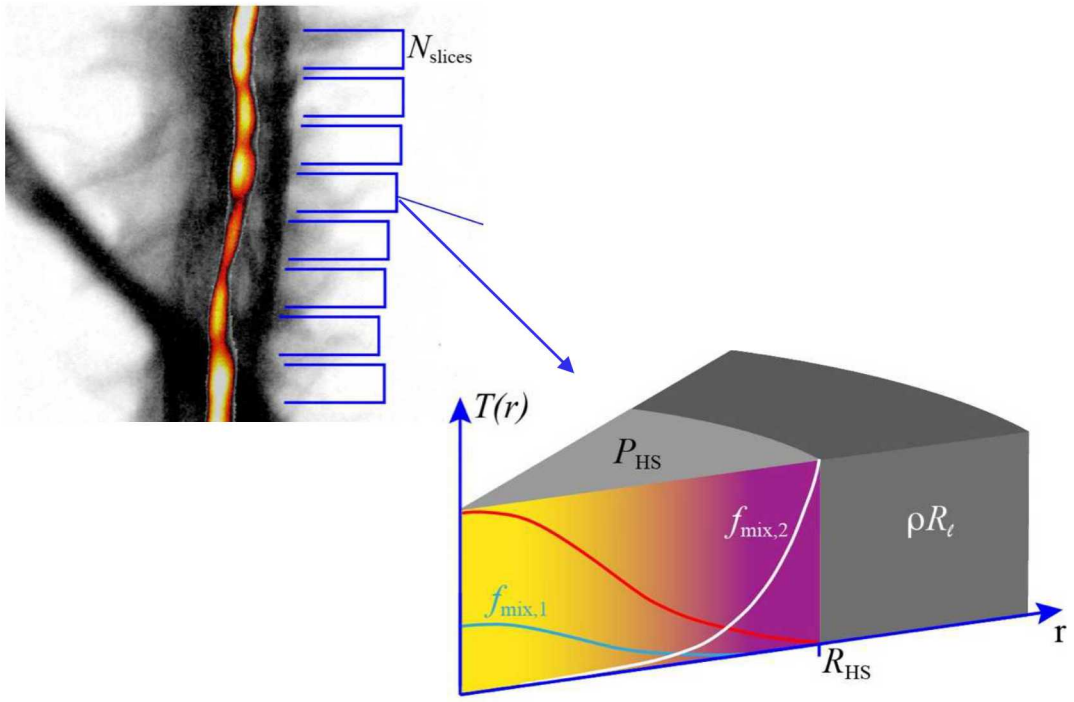

X-ray Emission:

$$\epsilon_\nu = A_{f-f} e^{-\rho R_\ell \kappa_\nu} \tau_b P_{HS}^2 \frac{g_{FF}\langle Z\rangle}{(1+\langle Z\rangle)^2} \sum_i f_i \tilde{j}_i \frac{e^{-h\nu/T}}{T^{5/2}}$$

$$\tilde{j}_i \equiv \frac{j_i}{j_D} = Z_i^2 + \frac{A_{f-b}}{A_{f-f}} \frac{Z_i^4}{T} e^{RyZ_i^2/T}$$

Neutron Emission:

$$\epsilon_E = \frac{P_{HS}^2 \tau_b}{1+\delta_{1,2}} \frac{f_1 f_2 \langle\sigma v\rangle}{(1+\langle Z\rangle)^2 T_i^2} I_o(E)$$

$$^*I_o(E) = e^{\frac{-2\bar{E}}{\sigma^2}(\sqrt{E}-\sqrt{\bar{E}})^2}$$

Assumptions:

- Each slice has its own independent parameters characterizing a static, isobaric hot spot surrounded by a liner
- Ideal gas EOS: $P_{HS} = (1+\langle Z\rangle) n_i k_B T$
- All elements have same burn duration
- Electron and ion temperatures are equal
- X-ray emission is dominated by continuum (BF & FF)

Basic Model Parameters	Global/hyper Parameters
$\{T_i\} = \{T_e\}$	Z_{mix}
$\{\rho R_\ell\}$	τ_{burn}
$\{P_{HS}\}$	h_{HS}
$\{f_{mix}\}$	T_{exp}
$\{R_{HS}\}$	

*Ballabio et al., NUCLEAR FUSION, Vol. 38, No. 11 (1998)

Analysis is performed using Bayesian Parameter estimation to determine the most likely hotspot parameters

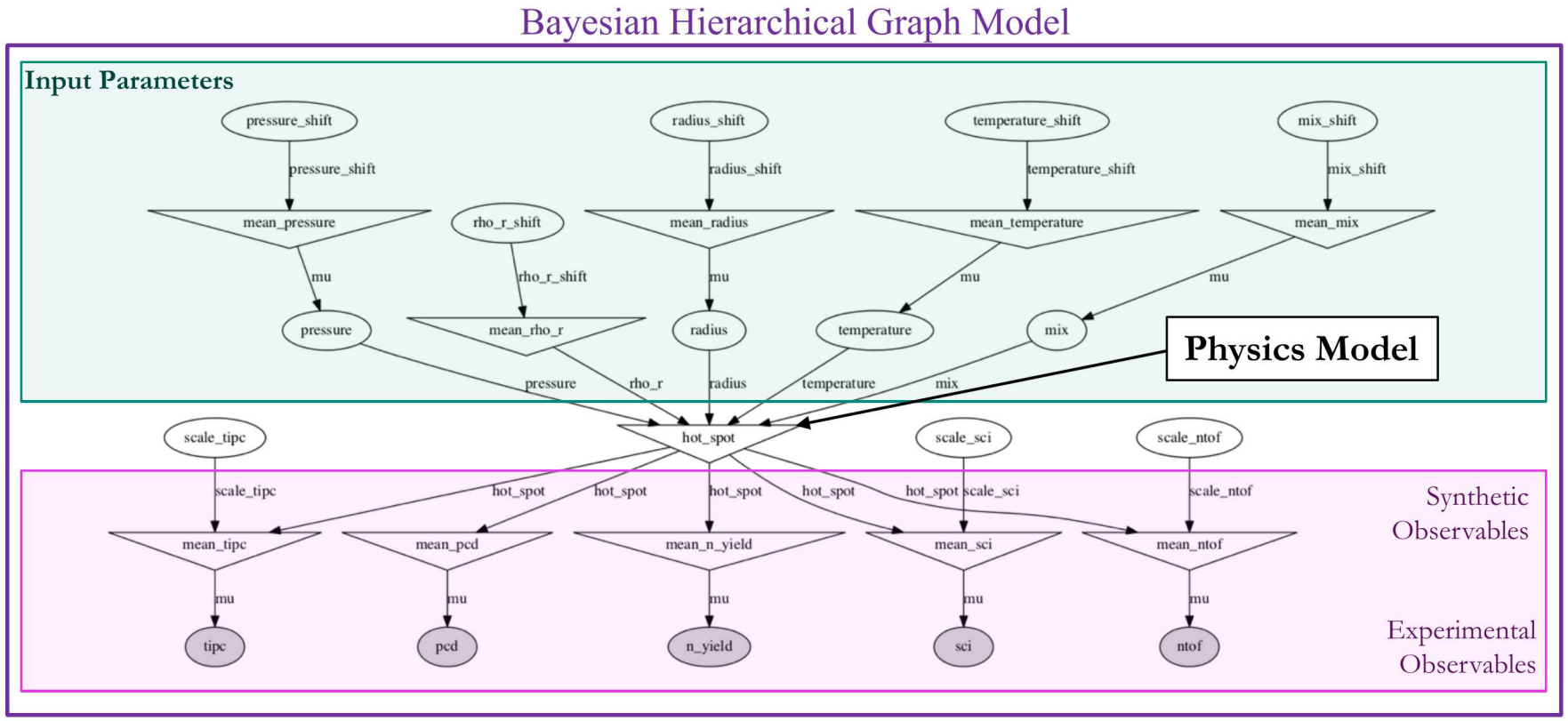

- Bayesian parameter estimation is a well-established technique used in a variety of fields*
- Analysis can be used to infer most likely parameters, correlations between model parameters and/or data
- Can compute value of information to determine which data constrain which parameters and how well

*U. Von Toussaint, Rev. Mod. Phys. Vol. 83 (2011)

Bayesian Parameter estimation is an iterative process that updates our assumptions based on observables

Bayes' Theorem

$$\mathcal{P}(\overline{\mathbf{m}}|\overline{\mathbf{d}}, A) = \frac{\mathcal{P}(\overline{\mathbf{d}}|\overline{\mathbf{m}}, A)\mathcal{P}(\overline{\mathbf{m}}|A)}{\mathcal{P}(\overline{\mathbf{d}}|A)}$$

Likelihood

$$\mathcal{P}(\overline{\mathbf{d}}|\overline{\mathbf{m}}, \mathcal{A}) \propto \prod_{i=1}^{N} \exp\left(-\frac{(\mathcal{F}_i(\overline{\mathbf{m}}) - d_i)^2}{2\sigma_i^2}\right)$$

Prior Distribution

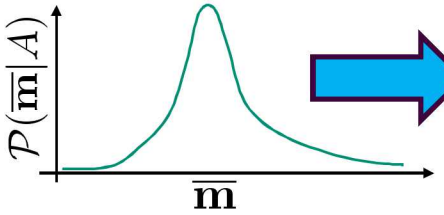

Experimental Data

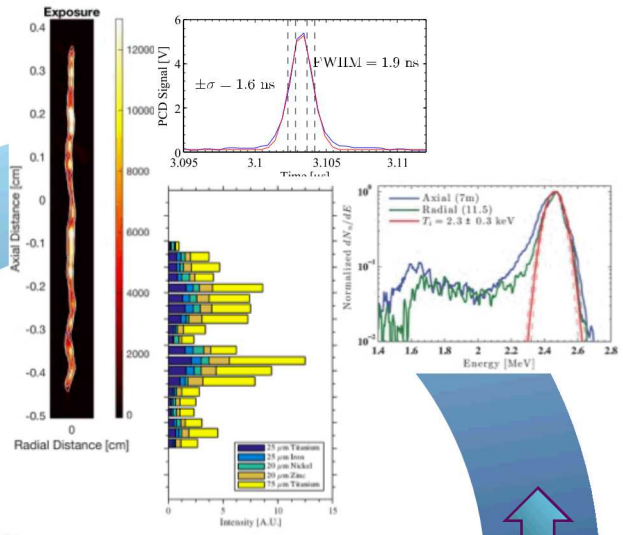

Proposed Stagnation Conditions

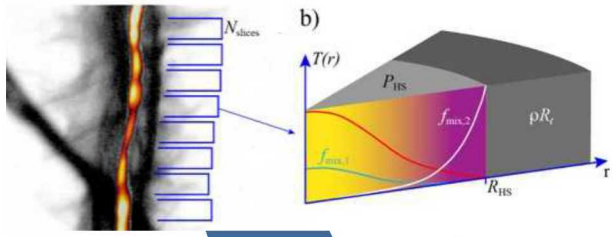

Synthetic Data

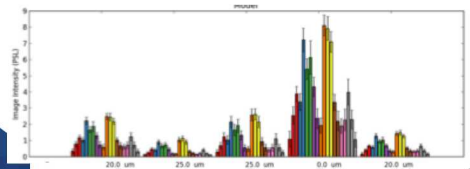

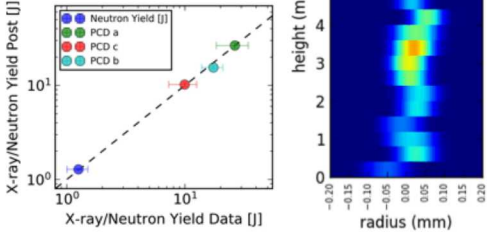

Model Parameters

$$\overline{\mathbf{m}} = \begin{cases} P_{\mathrm{HS}} \\ T \\ f_{\mathrm{mix}} \\ R_{\mathrm{HS}} \\ \rho R_\ell \end{cases}$$

Posterior Distribution

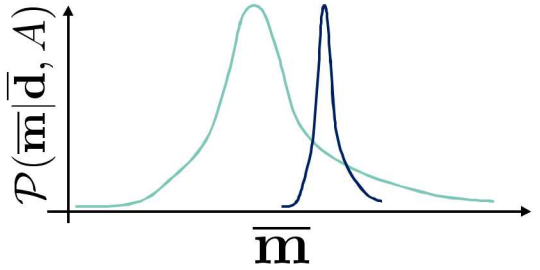

Outputs/Benefits:

- most likely parameter values
- confidence intervals
- correlations
- Value of information

Optimization Procedure

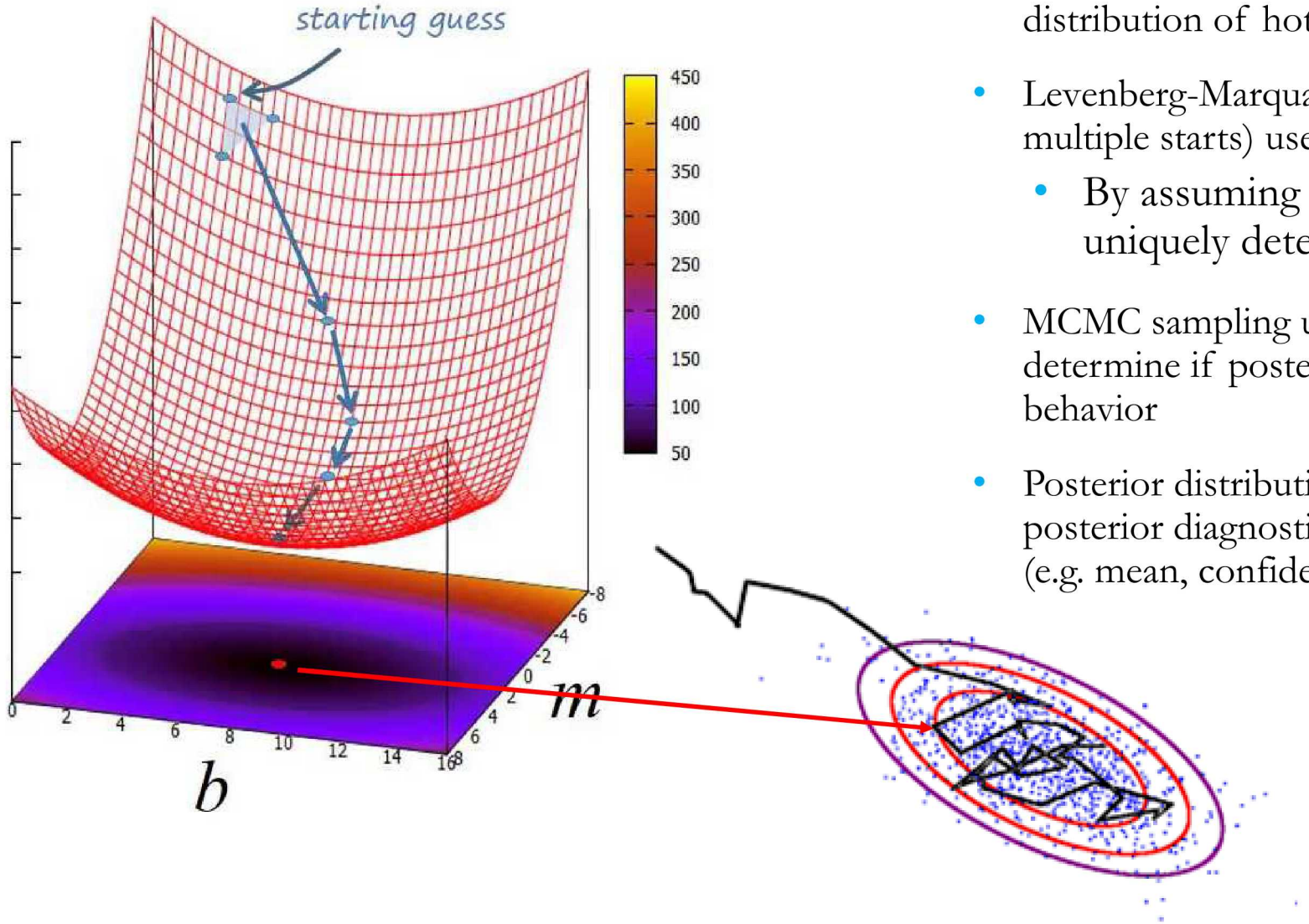

- Prior distribution is sampled to build the prior distribution of hotspot and diagnostic realizations
- Levenberg-Marquardt optimization (with optional multiple starts) used to determine the MAP solution
  - By assuming a Gaussian form this solution uniquely determines the posterior
- MCMC sampling used to refine the solution and determine if posteriors show any non-linear behavior
- Posterior distribution is sampled to form the posterior diagnostic and model parameter statistics (e.g. mean, confidence interval, etc.)

1D model Test case

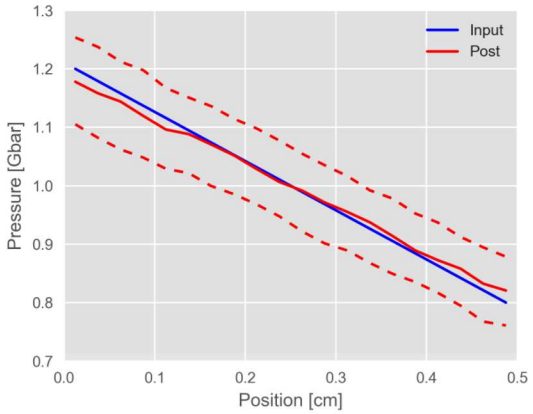

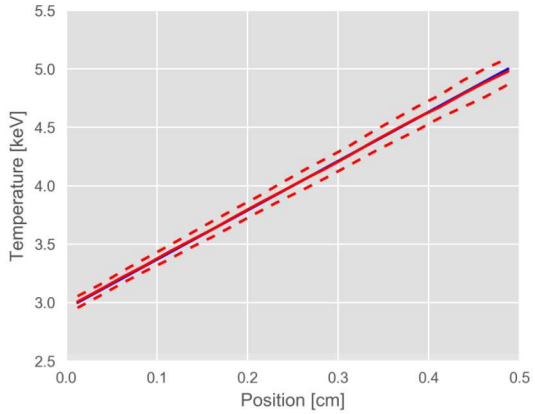

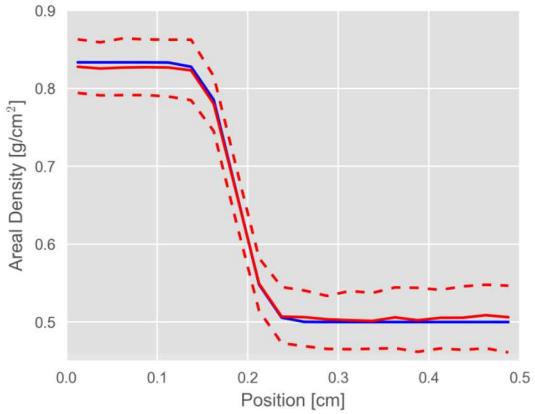

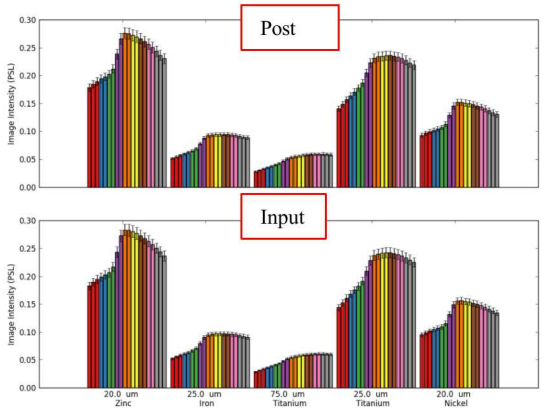

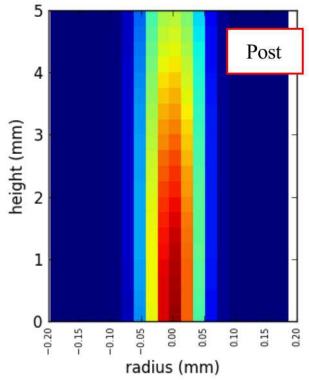

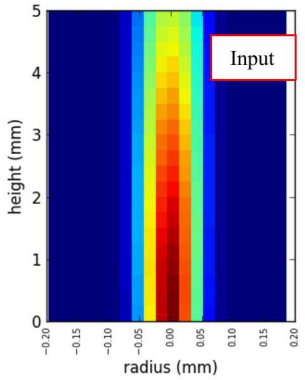

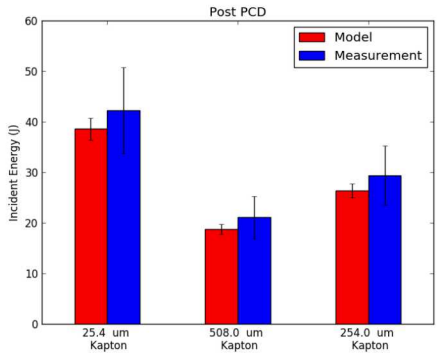

- Constructed a test case that exercises multiple parameters simultaneously
- Prescribed variations in P, T, and radius (all accurately determined)
- Mix and liner areal density are determined, but with large confidence intervals

Method has been successfully tested on 1D GORGON simulation data

What is the meaning of the model parameters in the presence of significant time evolution?

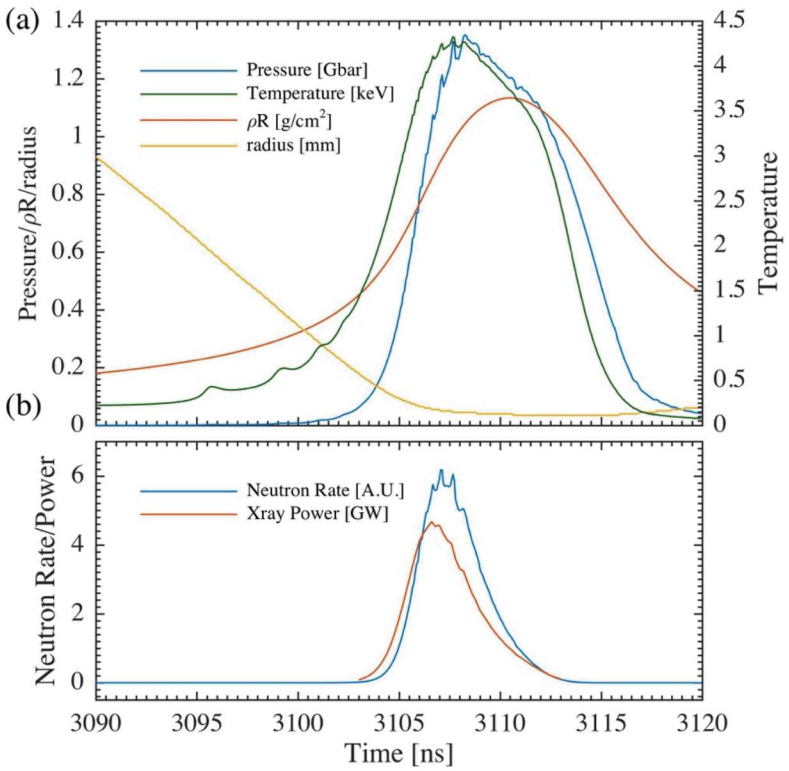

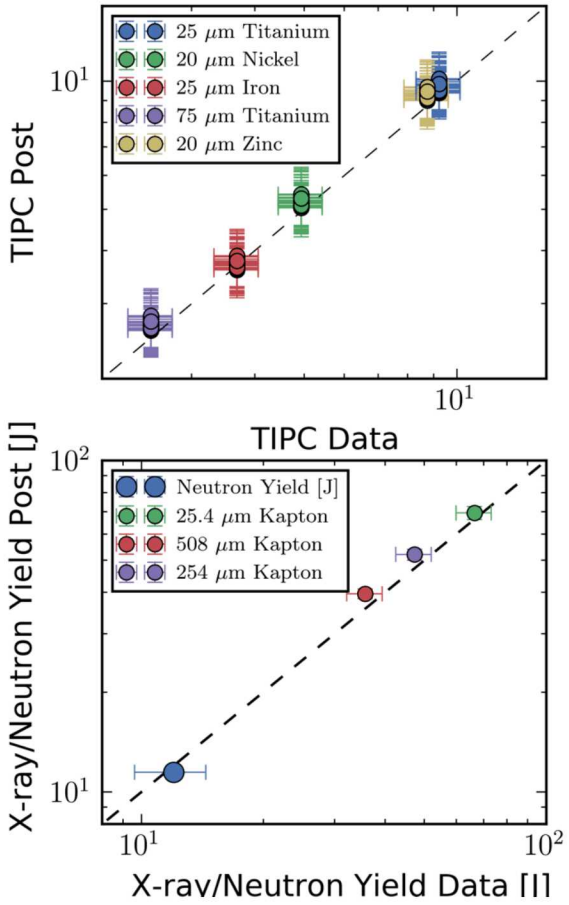

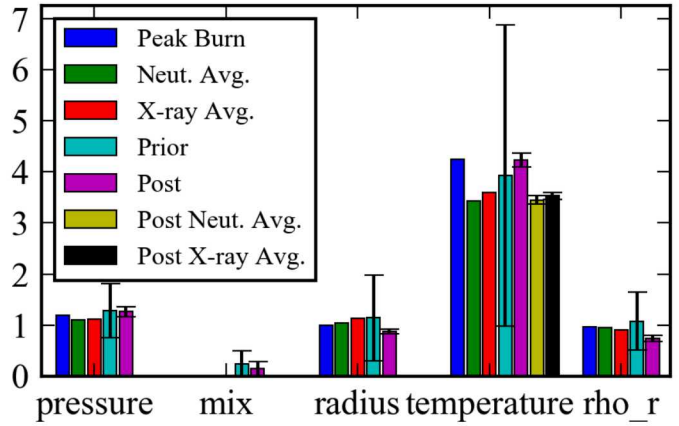

- The inversion is able to recover a high fidelity solution to the 1D GORGON simulation
- Inferred quantities correspond closely to simulated values at peak burn
- Inferred areal density is low, likely due to use of cold opacity in model
- Inferred radius is low, due to model definition

This tool is used to quantify the impact of new diagnostic information

Using synthetic test cases, we can demonstrate the utility of adding new diagnostic information

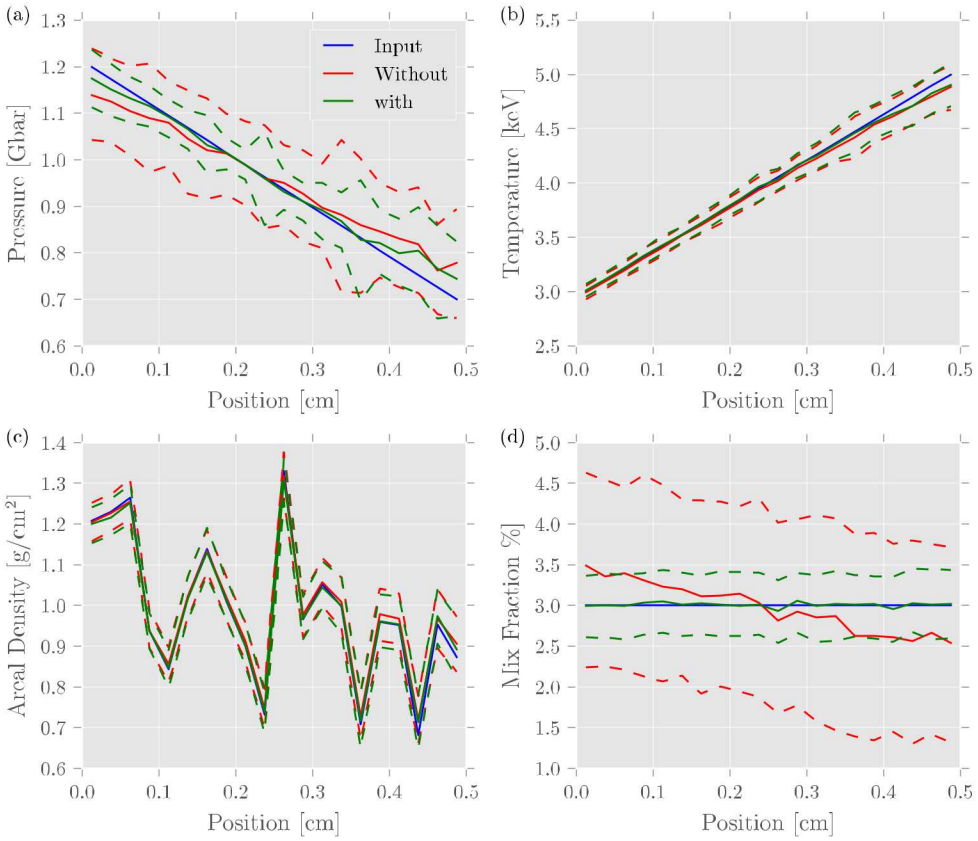

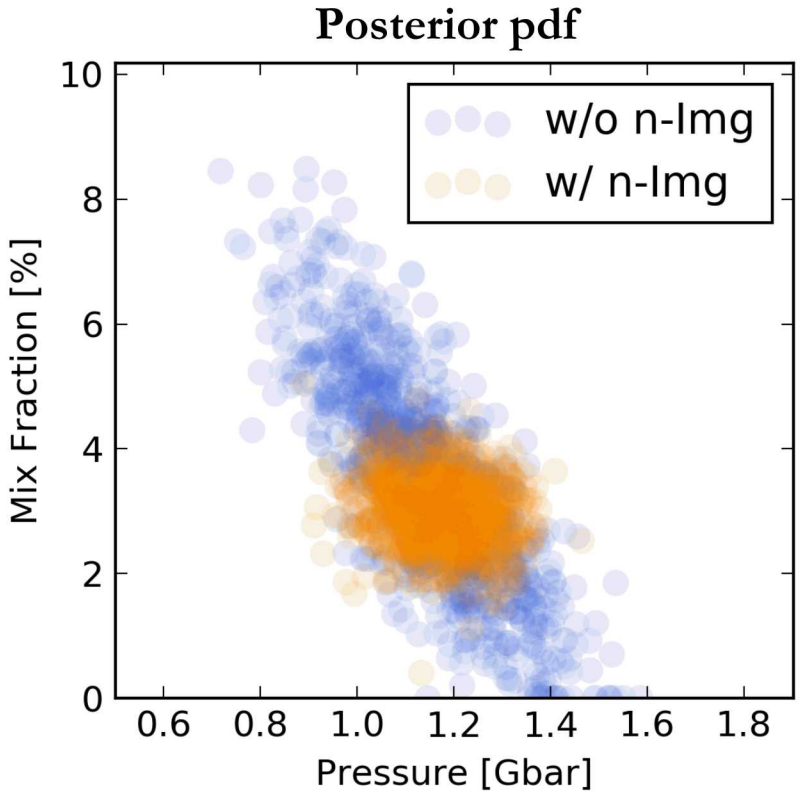

Performing the inversion with and without a 1D neutron image shows a dramatic change in the results

Without the image, there is significant correlation between the pressure and mix parameters

The neutron image breaks this degeneracy, improving the inference and reducing the C.I. on multiple parameters

We are able to use this analysis shows that low mix is strongly correlated with high pressure

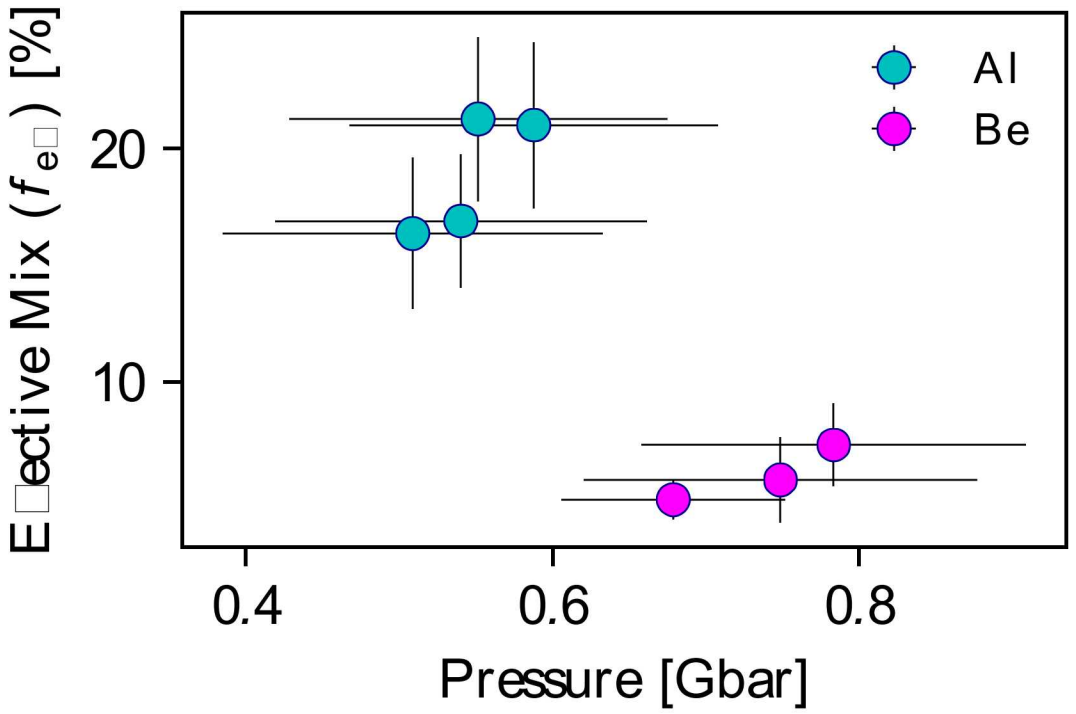

- This analysis determines the stagnation pressure and an *effective* mix fraction (assuming mix is 100% Be)
- The Be cushion shots have, on average
  - 3x less effective mix fraction
  - ~40% higher pressure
- The average hotspot energy is ~50% higher in the Be cushion experiments

$$\langle E_{\mathrm{HS}}^{\mathrm{Al}} \rangle = \langle \frac{3}{2} P_{\mathrm{HS}} V_{\mathrm{HS}} \rangle \approx 7.6 \text{ kJ} \qquad \langle E_{\mathrm{HS}}^{\mathrm{Be}} \rangle = \langle \frac{3}{2} P_{\mathrm{HS}} V_{\mathrm{HS}} \rangle \approx 11.4 \text{ kJ}$$

Use of a dielectric coating on the liner leads to a more uniform stagnation and elevated pressure

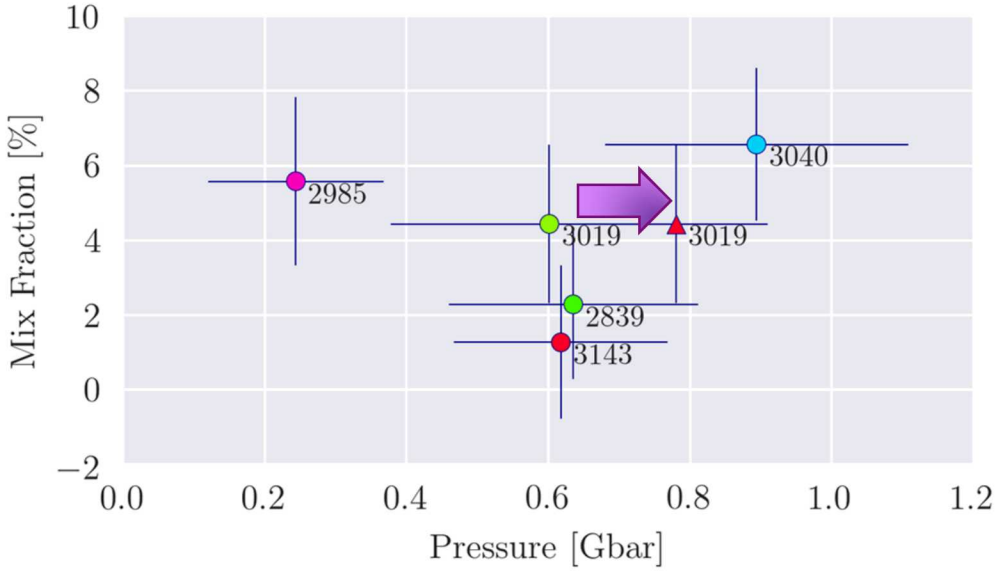

uncoated coated

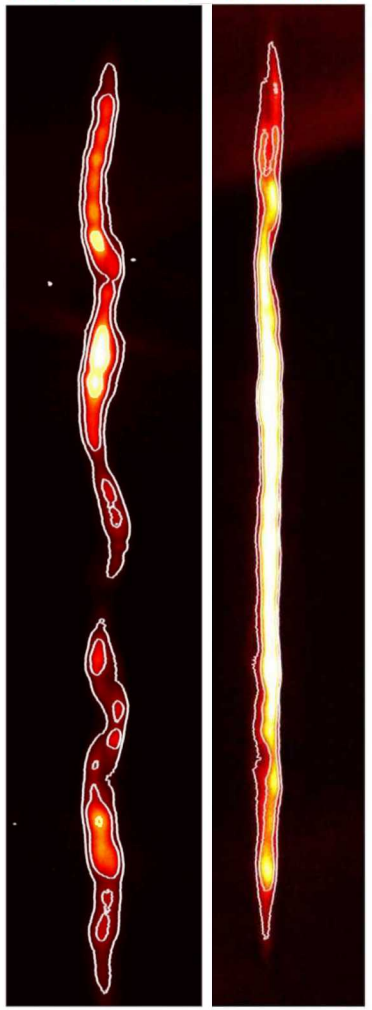

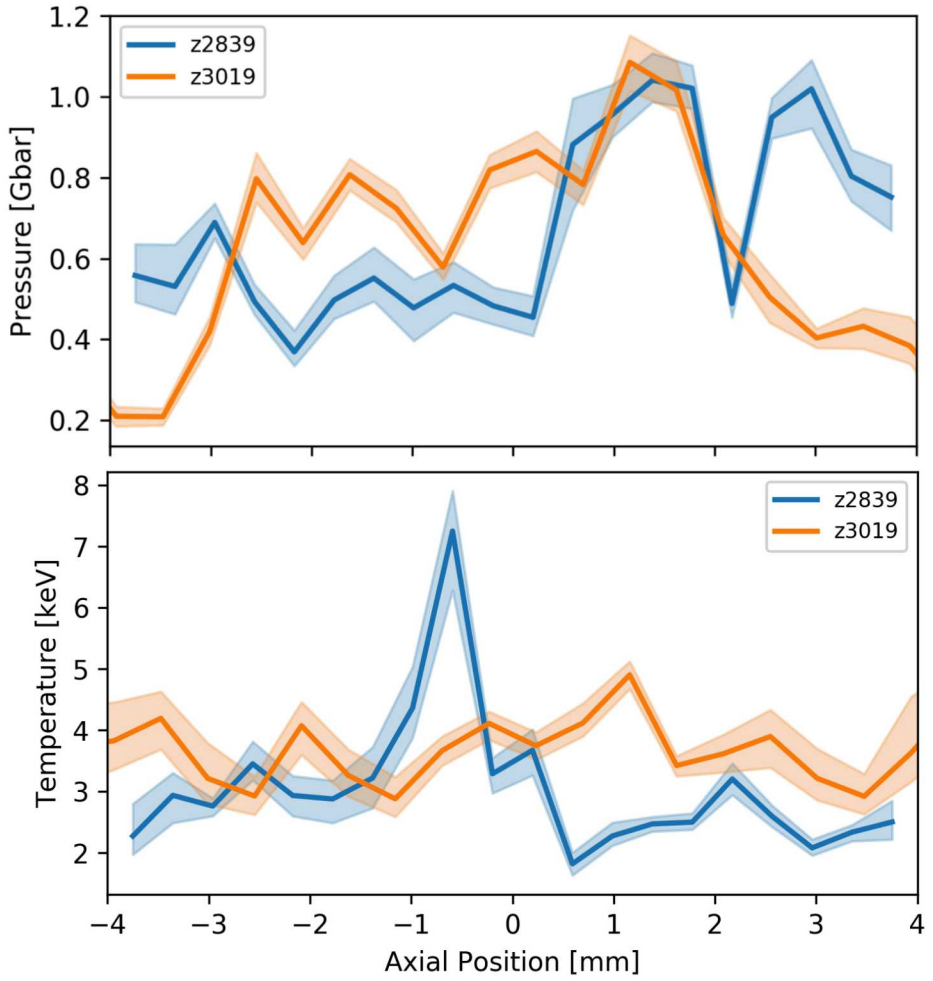

- Stagnation of coated target exhibits more uniform temperature, radius, and liner areal density than uncoated experiments
- Stagnation column is considerably straighter
- points to improved stability at stagnation
- Solution appears to lack the systematic swings that plague more structured data sets

K.J. Peterson et al., Phys. Plasmas 20, 026305 (2013)

Comparison with 3D GORGON simulations shows the volume averaged quantities agree well

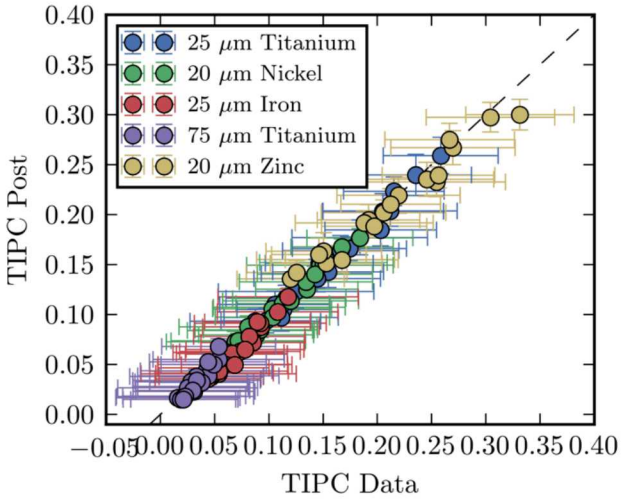

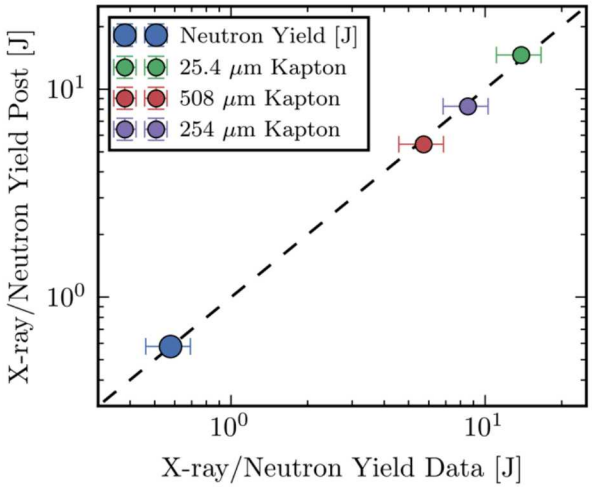

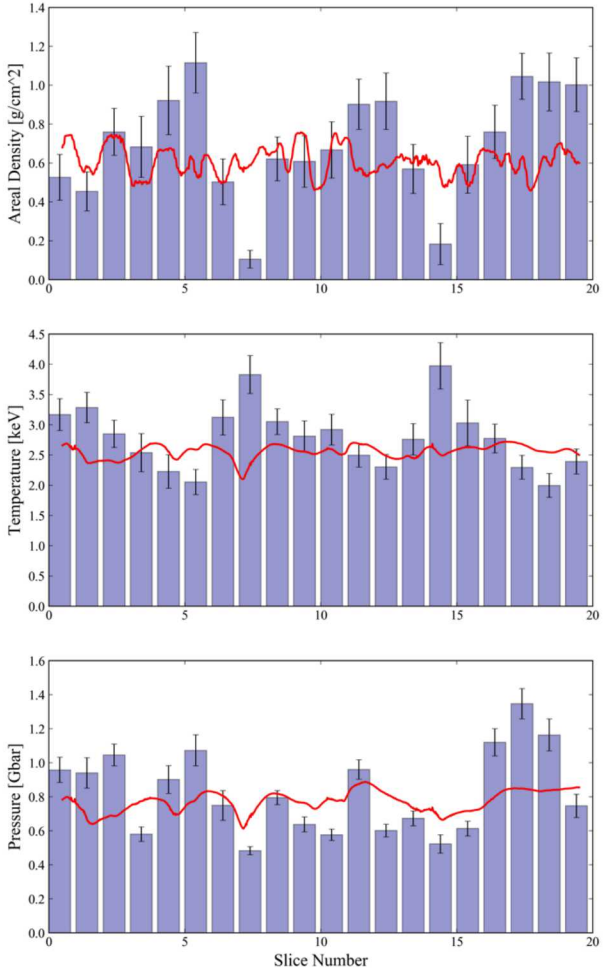

$$\langle \rho R_{\mathrm{m}} \rangle = 0.48 \pm 0.28 \ \mathrm{g/cm^2}$$
$$\langle \rho R_{\mathrm{G}} \rangle = 0.6 \ \mathrm{g/cm^2}$$

$$\langle T_{\mathrm{m}} \rangle^{\mathrm{burn}} = 2.67 \pm 0.4 \ \mathrm{keV}$$
$$\langle T_{\mathrm{G}} \rangle^{\mathrm{burn}} = 2.6 \ \mathrm{keV}$$

$$\langle P_{\mathrm{m}} \rangle = 0.75 \pm 0.2 \ \mathrm{Gbar}$$
$$\langle P_{\mathrm{G}} \rangle = 0.77 \ \mathrm{Gbar}$$

$$\langle f_{\mathrm{mix,G}} \rangle = 3 \ \%$$
$$\langle f_{\mathrm{mix,m}} \rangle = 2.5 \pm 1 \ \%$$

But, large discrepancies are seen in the local quantities!!

Further investigation shows significant bias in the solution when highly structured stagnation is considered

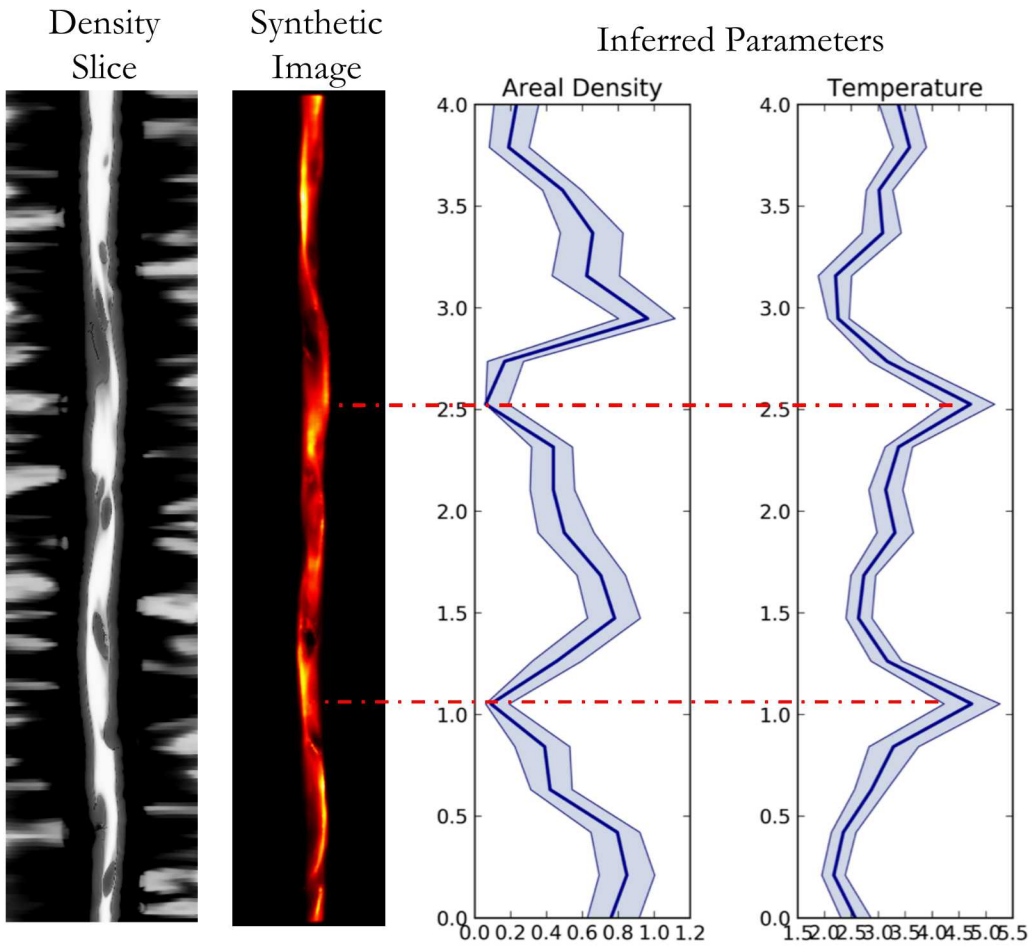

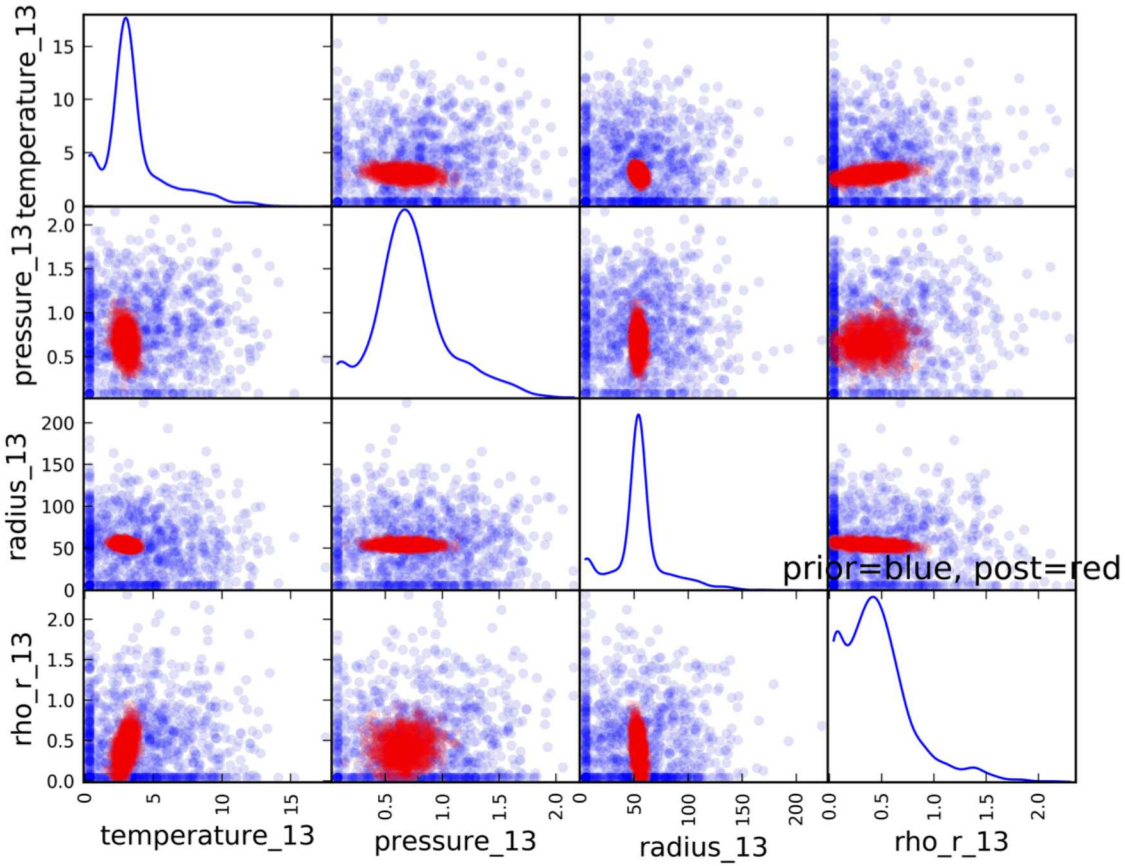

- Temperature, liner areal density, and pressure are all correlated
- Effect is worst at or near highly asymmetric portions of the column

Analysis from z2839, the canonical MagLIF experiment

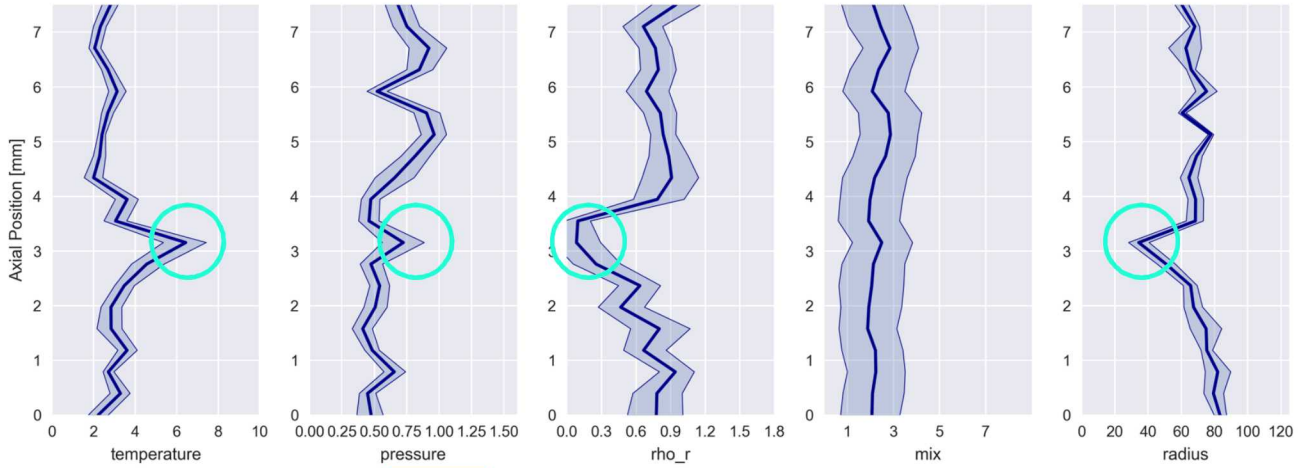

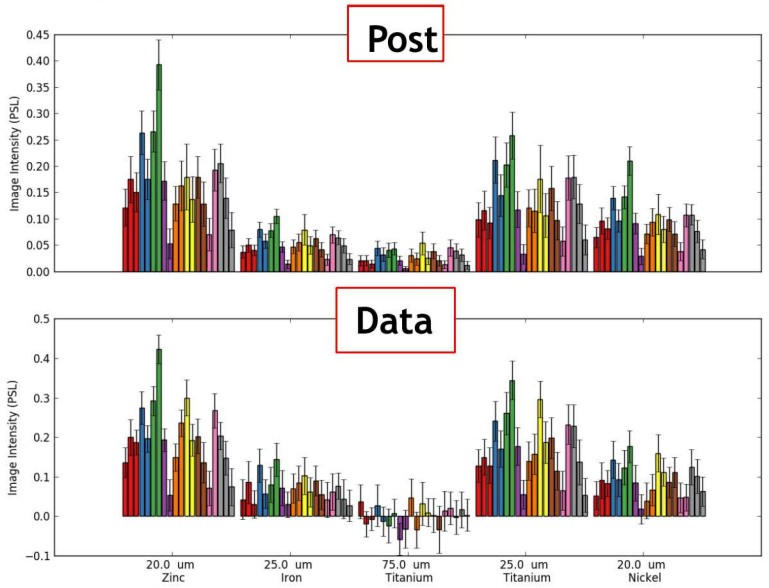

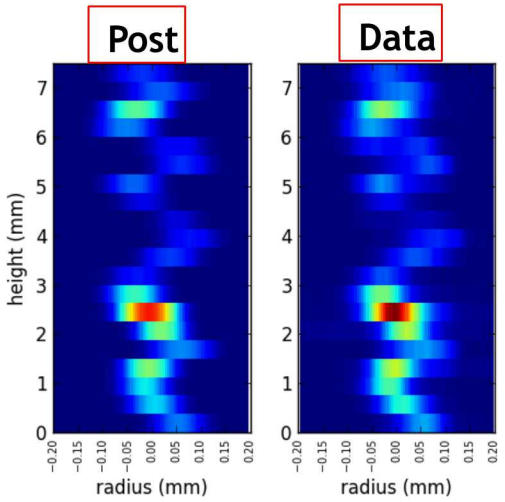

$$Y_{\mathrm{DD}}^{\mathrm{meas}} = 3.2 \times 10^{12} \pm 20\%$$
$$Y_{\mathrm{DD}}^{\mathrm{post}} = 3.1 \times 10^{12} \pm 10\%$$

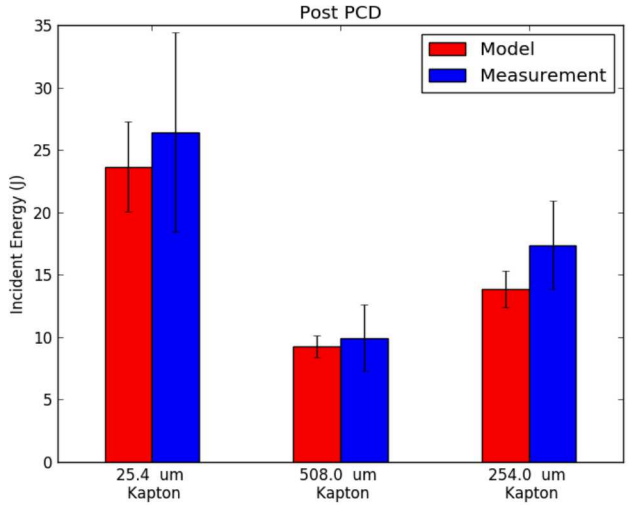

- One isolated region of obvious pathological behavior
- Otherwise, solution appears reasonably well behaved
- For the moment, we will use the inversion to construct average stagnation quantities

The biases are believed to be related to the three dimensional nature of the stagnation

Visualizations from GORGON Calculation at Peak Burn

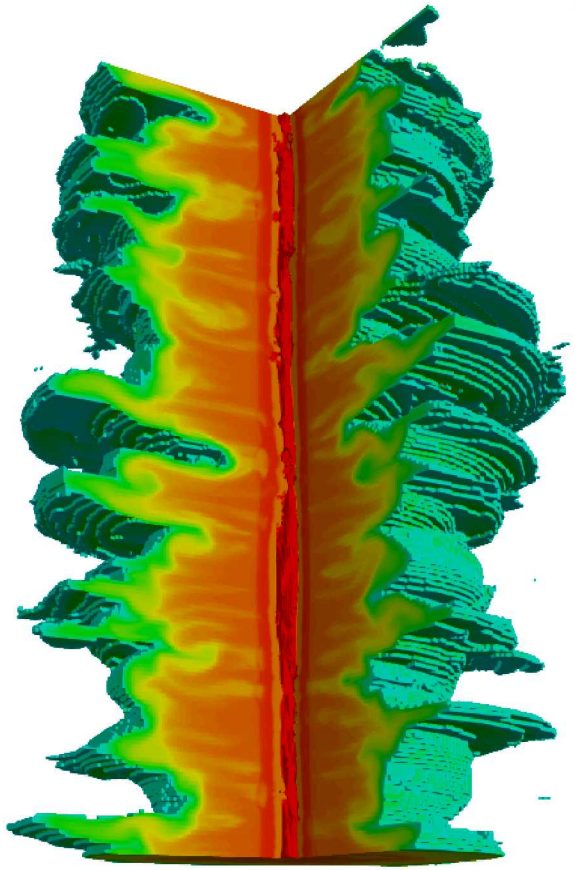

Density Map

Density Slice

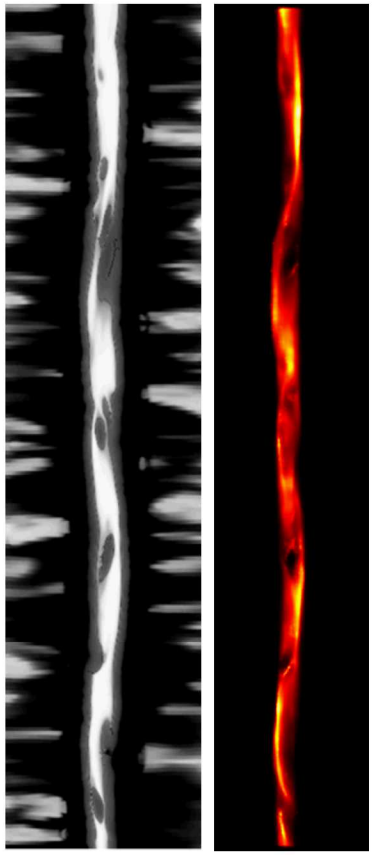

Synthetic Image

- Inability to match asymmetric indicates deviation from cylindrical symmetry
- This puts an artificial bias on the volume, which cascades through the correlations in the model and diagnostics to bias all quantities
- The large, anti-correlated swings in areal density and temperature are symptoms of this

Cross Section

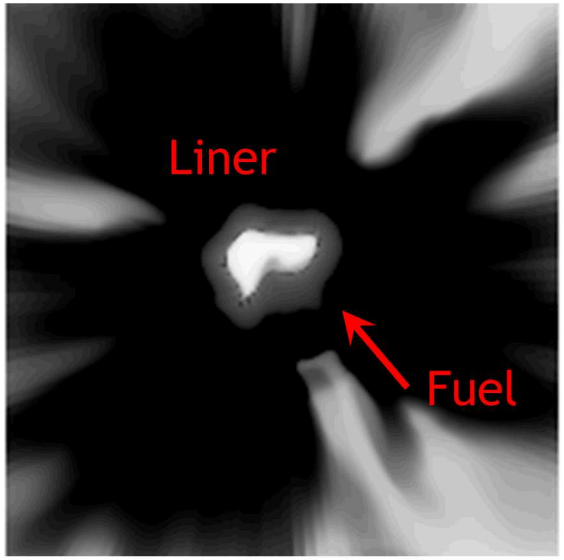

Calculations courtesy C. Jennings

Significant asymmetries are seen in the fuel morphology

We have developed two 3D models with different shape parameterizations to overcome this bias

Legendre Expansion

$$R(\theta) = R_o \sum_{\ell=0}^{2} a_\ell P_\ell(cos(\theta - \phi))$$

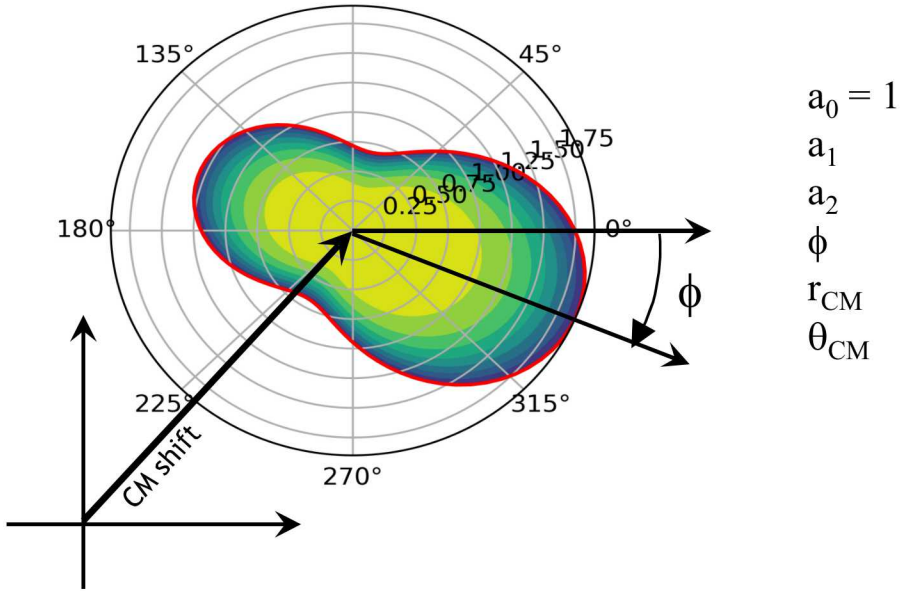

$a_0 = 1$
a_1
a_2
ϕ
r_{CM}
θ_{CM}

KDE Expansion

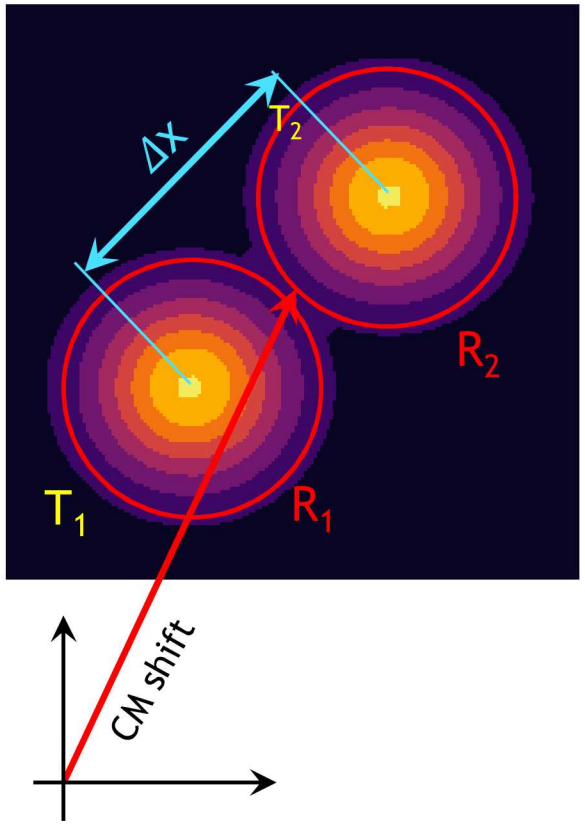

- Temperature parameters control the relative peaks of the two modes
- Radius parameters control the relative size of each mode

Temperature profile defined by one of two kernels

Power-Law Kernel

$$K(\mathbf{x}|\mathbf{X}, R) = 1 - T_{\text{frac}} \left(\frac{\sqrt{(\mathbf{x} - \mathbf{X})^2}}{R} \right)^p \quad T_{\text{frac}} = \frac{T_{\text{peak}}}{T_{\text{wall}}}$$

Super-Gaussian Kernel

$$K(\mathbf{x}|\mathbf{X}, R) = \exp\left(- \left(\frac{1}{2} \frac{(\mathbf{x} - \mathbf{X})^2}{\sigma^2} \right)^p \right) \quad \sigma = \frac{2}{3} R$$

The addition of shape and CM shift parameters requires that we have an additional viewing angle in our diagnostics

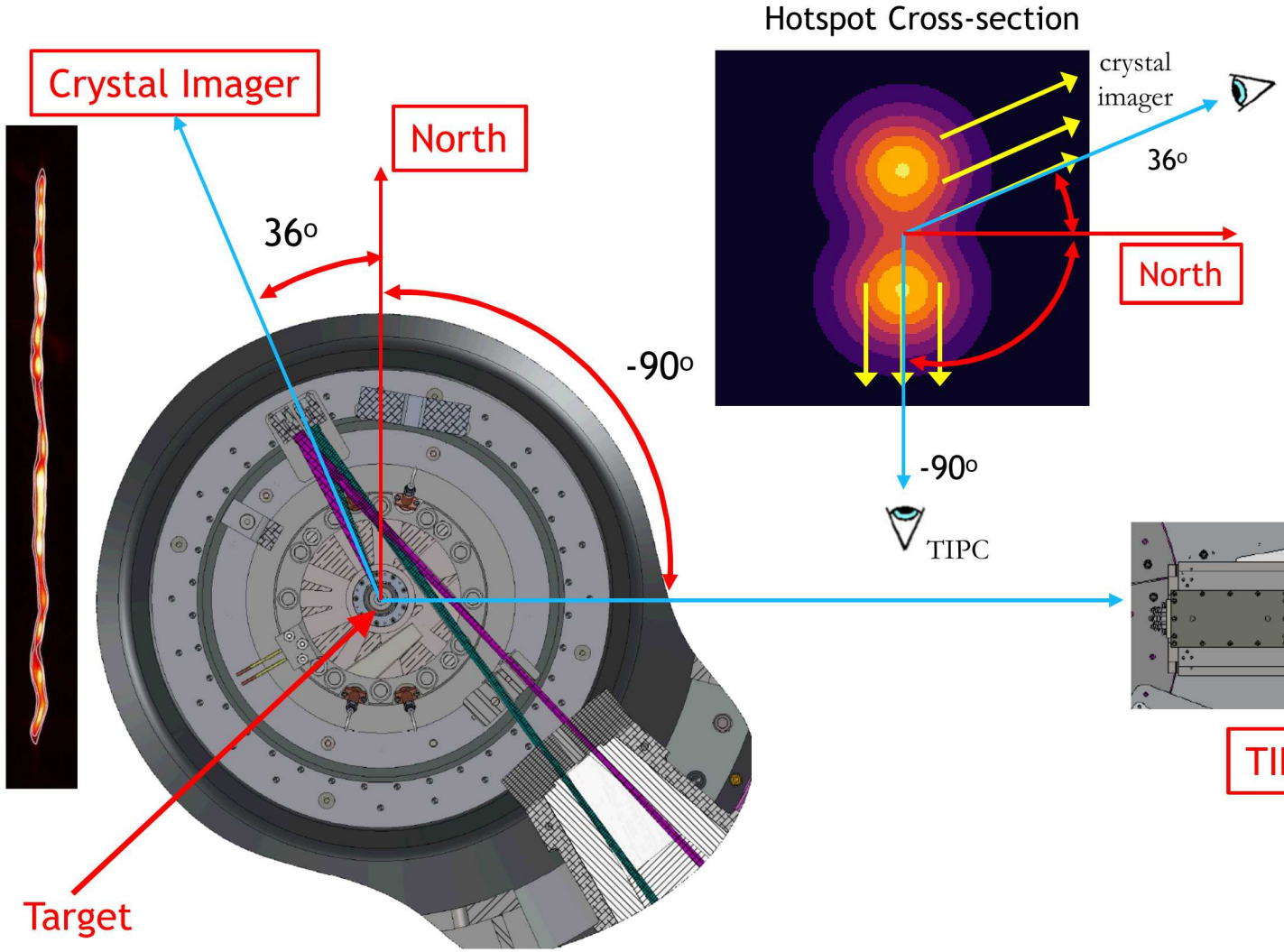

Top view of Load Region

Original model treats TIPC as a 1D imager

Now, we exploit the full images as well as the viewing angles of the crystal imager and TIPC constrain the new parameters

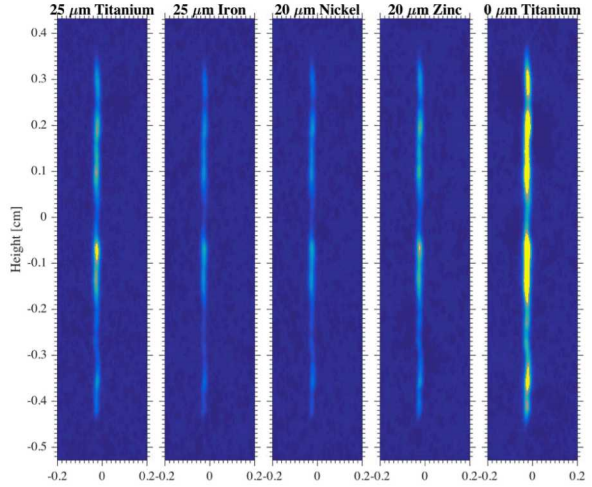

But TIPC has much worse resolution than the crystal imager

Unfortunately, incorporating the new parameters has made the optimization significantly more challenging

correct answer: x_cm = -50, y_cm = 50, a1 = 1.0

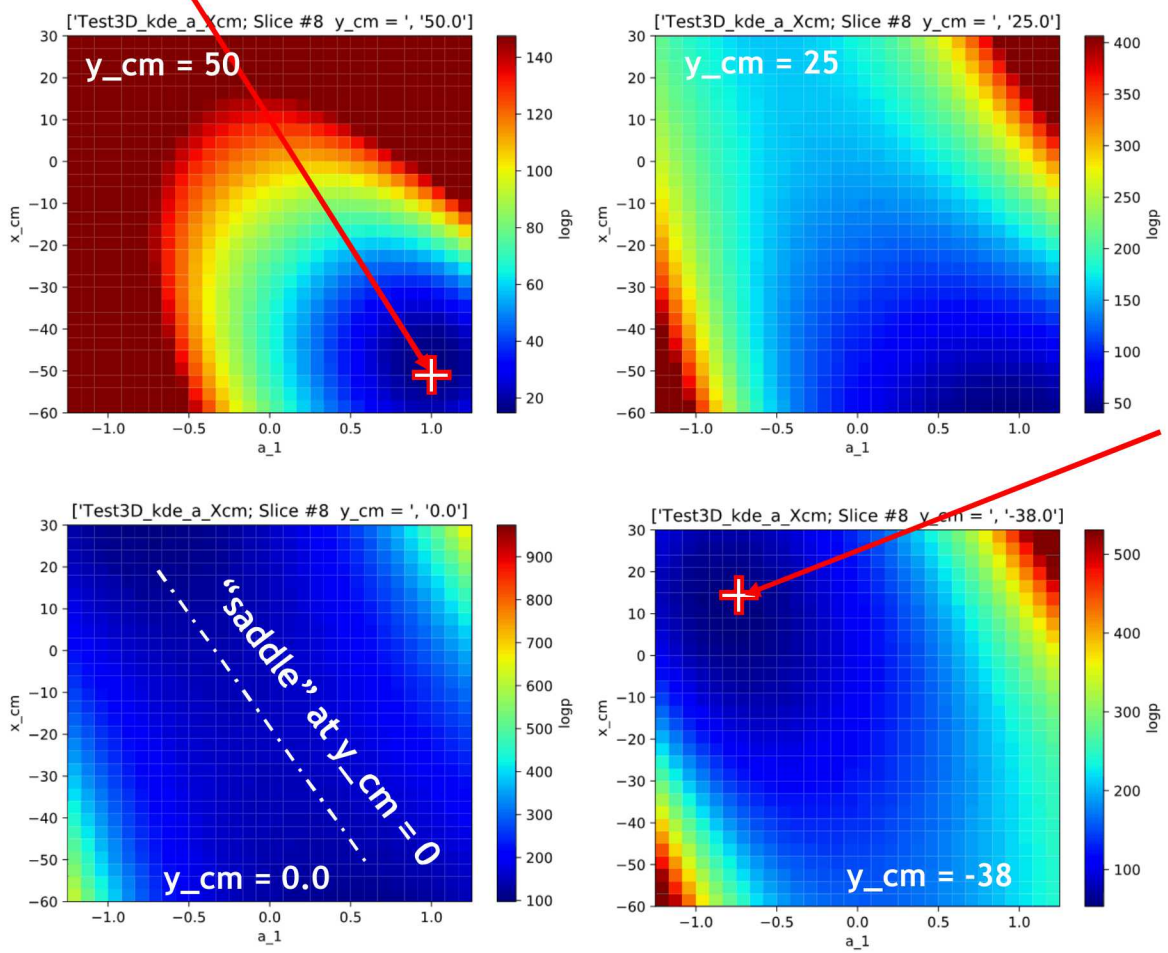

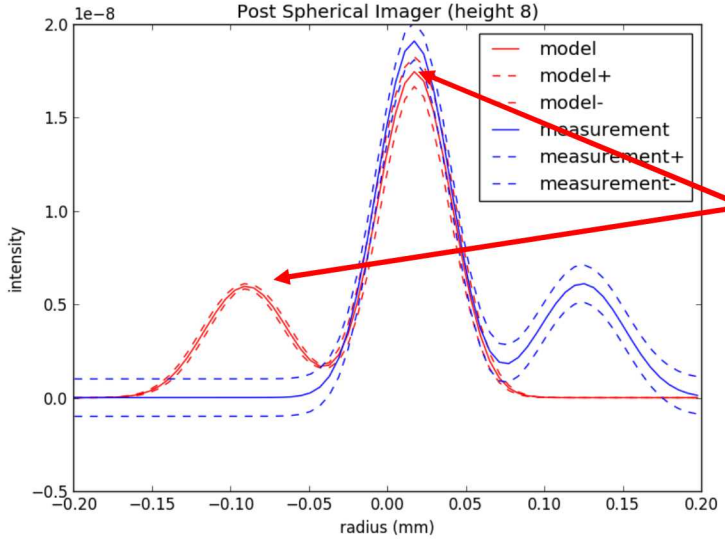

The wrong "polarity" of the modes, and the algorithm minimizes the difference with the central lobe

Inferred answer: x_cm = ~20, y_cm = ~38, a = -0.75

- Each plot shows the objective as a function of x_cm and a1 for different values if y_cm
- The algorithm needs to be seeded with a positive or negative bias in X_cm, or it will stall.
- That bias introduces a bias in a1

Conclusions

We have used the Bayesian technique to constrain stagnation quantities using multiple diagnostics simultaneously

This has been used to uncover trends in the data, guide target designs, and help motivate a new instrument

Increasing the fidelity of the physics model shows promise to overcome some challenges but is an active area of work